

The metal-insulator transition in amorphous $\text{Si}_{1-x}\text{Ni}_x$: Evidence for Mott's minimum metallic conductivity

A. Möbius,^{1*} C. Frenzel,¹ R. Thielsch,^{1,2} R. Rosenbaum,³ C.J. Adkins,⁴ M. Schreiber,⁵
H.-D. Bauer,¹ R. Grötzschel,⁶ V. Hoffmann,¹ T. Krieg,¹ N. Matz,¹ H. Vinzelberg,¹ and
M. Witcomb⁷

¹*Institute for Solid State and Materials Research Dresden, D-01171 Dresden, Germany,*

²*Fraunhofer Institute for Applied Optics and Precision Mechanics, Schillerstr. 1, D-07745 Jena, Germany,*

³*Tel Aviv University, School of Physics and Astronomy, Raymond and Beverly Sackler Faculty of Exact Sciences, Ramat Aviv, 69978, Israel,*

⁴*Cavendish Laboratory, Madingley Road, Cambridge CB3 0HE, UK,*

⁵*Technical University Chemnitz, Institute of Physics, D-09107 Chemnitz, Germany,*

⁶*Research Center Rossendorf, Institute for Ion Beam Physics and Materials Research, D-01314 Dresden, Germany,*

⁷*University of the Witwatersrand, Electron Microscope Unit, Private Bag 3, Wits, 2050, South Africa*

(October 24, 2018)

Abstract

We study the metal-insulator transition in two sets of amorphous $\text{Si}_{1-x}\text{Ni}_x$ films. The sets were prepared by different, electron-beam-evaporation-based technologies: evaporation of the alloy, and gradient deposition from separate Ni and Si crucibles. The characterization included electron and scanning tunneling microscopy, glow discharge optical emission spectroscopy, energy dispersive X-ray analysis, and Rutherford back scattering. Investigating the logarithmic temperature derivative of the conductivity, $w = d \ln \sigma / d \ln T$, we observe that, for insulating samples, $w(T)$ shows a minimum, increasing at both low and high T . Both the minimum value of w and the corresponding temperature seem to tend to zero as the transition is approached. The analysis of this feature of $w(T, x)$ leads to the conclusion that the transition in $\text{Si}_{1-x}\text{Ni}_x$ is very likely discontinuous at zero temperature in agreement with Mott's original views.

71.30.+h, 71.23.Cq, 68.55.-a, 81.15.-z

Typeset using REVTeX

*e-mail: a.moebius@ifw-dresden.de

I. INTRODUCTION

Metal-insulator transitions (MIT) in disordered systems have attracted much interest, theoretical as well as experimental, for forty years. Milestones on this way were the concepts of Anderson localization [1], of minimum metallic conductivity [2], the scaling theory of localization [3], and the renormalization group approach incorporating the electron-electron interaction into localization theory [4–6]; for surveys see Refs. [7–12].

Nevertheless, important questions have not been finally settled yet: Contrary to Mott’s prediction of a finite minimum metallic conductivity, the scaling theory of localization predicts continuity of the conductivity at the MIT for three-dimensional systems. That means, for the transition being approached from the metallic side at zero temperature, $T = 0$, the conductivity, $\sigma(T, x)$, is expected to vanish continuously according to

$$\sigma(0, x) \propto |x - x_c|^\nu, \quad (1)$$

where x stands for the control parameter (concentration / magnetic field / stress ...), and x_c for its value at the MIT. The value of the critical exponent ν has been a subject of controversial debate since its first measurements, see e.g. Refs. [13–18]. However, several studies have pointed to inconsistencies of the zero-temperature extrapolations inherent in the critical-exponent determination [8,12,18–22]. These problems could, of course, arise from quantitative failure of the extrapolation formulae used or from imperfections of samples or σ and T measurements, but they could also be caused by discontinuity of $\sigma(0, x)$ at x_c [8,12], in which case the critical-exponent puzzle would simply be an artifact arising from unphysical fitting. The unclear situation described is the main motivation of the present study.

The recent discovery of a sharp MIT in two-dimensional disordered systems [23–26] has drawn interest to this subject, too. The scaling theory of localization of non-interacting electrons [3] states that two-dimensional systems exhibit principally only activated conduction, and denies the existence of an MIT in this situation. Hence it does not describe nature in this case. This failure is a strong additional motivation to re-consider the applicability of that theory to the MIT of three-dimensional systems.

In greater detail, the critical step of most of the recent studies of the MIT in three-dimensional disordered systems is the zero-temperature extrapolation, that is the determination of the limit $\sigma(T \rightarrow 0, x)$, for samples close to the MIT. This extrapolation can be based either on a microscopic theory, or on an empirically found relation supposed to be valid down to $T = 0$.

The extrapolation is particularly difficult if a strong, but non-exponential T dependence of σ is observed. In such a case, two interpretations are possible:

(i) The sample could be metallic. This situation is mostly analyzed in terms of theories by Altshuler and Aronov [27], or Newson and Pepper [28], which yield

$$\sigma(T, x) = a(x) + b(x) \cdot T^p \quad (2)$$

with $p = 1/2$, and $1/3$, respectively. The former theory models the superposition of electron-electron interaction and disorder, but it is a perturbation theory so that its applicability very close to the transition is at least questionable. The latter theory considers the T -dependent drop of the diffusion constant as the decisive variation, and yields a power law with exponent

1/3 for $x = x_c$.

(ii) The sample could exhibit activated conduction with the characteristic energy being smaller than the lowest experimentally accessible T . Thus it would have to be classified as insulating (at $T = 0$). If, as generally taken for granted, the characteristic energy vanishes continuously as $x \rightarrow x_c$, such an x region exists always, see Fig. 1. But, to the best of our knowledge, there is no appropriate microscopic theory for a related quantitative analysis available.

Unfortunately, when considering non-exponential $\sigma(T, x = \text{const.})$ dependences, many of the recent experimental studies analyze the data only in terms of (i). Moreover, to agree with Eq. (1), they presume that, as $x \rightarrow x_c$, the parameter a tends to 0. So it is not surprising that, when checking the applicability of Eq. (2) by considering the logarithmic derivative $d \ln \sigma / d \ln T$, doubts arose in several cases [19–22]: this quantity must vanish as $T \rightarrow 0$ for metallic samples, but, instead, often increases or stays approximately constant for the sample(s) assumed to be particularly close to the MIT. Therefore one should determine the MIT point by simultaneously considering both sides of the transition. Moreover, adjusting free parameters should be avoided to the largest possible extent. Such an approach was successful for amorphous $\text{Si}_{1-x}\text{Cr}_x$, see Refs. [29–33]. A simple phenomenological model of $\sigma(T, x)$ describing both sides of the MIT was constructed for that system starting from the detection of universal features in $\sigma(T, x)$, in particular from a scaling law for the T dependence in the activated region, $\sigma(T, x) = \sigma(T/T_0(x))$. However, annealing breaks this universality.

Due to the controversial situation described above, the aim of the present work is to analyze the $\sigma(T, x = \text{const.})$ relations close to the transition in as unbiased a way as possible, without fitting. For that we study amorphous silicon nickel films, $\text{a-Si}_{1-x}\text{Ni}_x$, prepared by electron beam evaporation. Thus, though the above discussion concerns a general problem occurring for an arbitrary type of the control parameter x , we focus now on a special case, and, in the following, x stands only for metal concentration in an amorphous alloy. In our study, we put emphasis on two methodical points: Firstly, we attach particular importance to the accuracy of the $d \ln \sigma / d \ln T$ values. Secondly, in order to avoid being misled by having used special preparation conditions, we investigate two series of samples, prepared by groups in Dresden and Tel Aviv.

There were several reasons for us to select $\text{a-Si}_{1-x}\text{Ni}_x$ for a detailed investigation:

- We were looking for an alloy which is sufficiently stable but differs substantially from $\text{a-Si}_{1-x}\text{Cr}_x$ which we had studied in detail previously [29–33]. According to the melting temperatures [34], $\text{a-Si}_{1-x}\text{Ni}_x$ can be expected to be rather stable, at least far more than $\text{a-Si}_{1-x}\text{Au}_x$ [35], or $\text{a-Ge}_{1-x}\text{Au}_x$ [36]. On the other hand, there is a deep eutectic point close to the MIT for the system Si-Cr, but not for Si-Ni [34]. Therefore, in a quenching experiment, it should be far more difficult to realize an amorphous structure close to the MIT in $\text{Si}_{1-x}\text{Ni}_x$ than in $\text{Si}_{1-x}\text{Cr}_x$ [37]. However, it is an open question, to what extent such considerations can be applied also to films produced by evaporation, or by sputtering.
- A second important difference between $\text{a-Si}_{1-x}\text{Ni}_x$ and $\text{a-Si}_{1-x}\text{Cr}_x$ concerns the character of the silicide which should be formed first in annealing the samples, cf. Refs. [38–40]: Si_2Ni is a metal, whereas Si_2Cr is a semiconductor with an indirect gap of roughly 0.3 eV [41].
- Conductivity studies (partly taking magnetoresistance into account) on hydrogenated and unhydrogenated sputtered $\text{a-Si}_{1-x}\text{Ni}_x$ films [42–45], as well as on polycrystalline films [46–48],

and on the influence of annealing [48,49] were available for comparison in the literature. Moreover, in the vicinity of the MIT, the electronic structure of $\text{a-Si}_{1-x}\text{Ni}_x$ was recently studied by XPS and UPS [50]. For $\text{a-Si}_{1-x}\text{Ni}_x\text{:H}$, a structure study [51], optical conductivity measurements [52], also under pressure [53], and electronic structure investigations by XPS and XES [54] were reported in the literature. Last but not least, some of the authors have gained detailed experience in trying fits of $\sigma(T)$ by conventional theories for $\text{a-Si}_{1-x}\text{Ni}_x$ samples prepared by electron-beam evaporation in Tel Aviv [55,56].

The present paper is organized as follows: Section II describes the sample preparation. Section III is devoted to the structural and chemical characterization, including an STM investigation. Section IV gives some experimental details of the conductivity measurements, whereas Section V analyses them in detail, and lists common and differing features of the two conductivity data sets. In Section VI, we discuss the qualitative character of the MIT. Finally, in Section VII, the conclusions from our findings are summarized.

II. FILM PREPARATION

We compare $\text{a-Si}_{1-x}\text{Ni}_x$ films, prepared by two different technologies. Both technologies are based on electron-beam evaporation, but they have specific advantages and disadvantages:

(A) Direct evaporation of SiNi alloys of various compositions from one crucible was used in Dresden, cf. Ref. [29]. In this case, changes of power cause changes of the composition of the films by modifying the vapor pressure ratio of the alloy components via the changed temperature of the ingot. Hence, the deposition rate has carefully to be held constant. Moreover, it is essential that the whole ingot is liquid; a check for contamination from the copper crucible showed it to be negligible. The x drift over the film thickness arising from Ni enrichment in the ingot material during evaporation is very small, see section III, since only a small portion of the ingot was evaporated in each cycle. Moreover, this drift is far smaller than the x difference between samples prepared in successive cycles using the same ingot, because the time which we waited until rate and pressure were stable is considerably larger than the deposition duration. Typical conditions were as follows: residual gas pressure during deposition $\approx 4 \cdot 10^{-6}$ mbar, and rate ≈ 2 nm/s.

(B) Co-evaporation of Ni and Si from separate crucibles was used in Tel Aviv to prepare in one deposition a whole set of samples. This method uses the varying incidence angles and distances to the sources to produce a composition gradient along a substrate. The film is then cut into narrow samples with their axes (the direction of current flow) perpendicular to the composition gradient [55]. This technique has two advantages: Composition determination is related to a geometrical measurement, and neighboring samples are prepared under almost identical conditions. Thus the random errors in studying x dependences can considerably be reduced. However, the crucial point is that one has to take great care to hold the ratio of the evaporation rates of both crucibles constant. The conditions were as follows: residual gas pressure during deposition $\approx 1 \cdot 10^{-5}$ mbar, and, for the samples close to the MIT, rate ≈ 0.8 nm/s; for more details see Ref. [55].

In the following, we refer to the samples prepared by technology A by the numbers 1 – 6, and to the samples produced by method B by the letters a – j. These two sample sets are labeled as A and B according to the preparation. Tables I and II give x , film thickness, and

conductivity at 300 and 4.2 K for the sets A and B, respectively. Samples 6 and i, both deep in the metallic region, and sample j, close to the MIT, are only included for comparison of x scales.

III. CHEMICAL AND STRUCTURAL CHARACTERIZATION

A. Composition

The chemical composition of the samples of set A was determined by Rutherford backscattering (RBS) at the Research Center Rossendorf within this work. For that we used Sigradur substrates (glassy carbon). We confirmed the consistency of these data by glow discharge optical emission spectroscopy (GDOES). Energy dispersive X-ray analysis (EDX) by means of a LINK AN10000 EDS system attached to a JSM-840 SEM was used in determining the composition for sample set B in Witwatersrand, South Africa, within Refs. [55,56]. The results of these analyses are given in Tables I and II.

In order to compare both x scales, we performed additional EDX analyses for samples 3, 6, f, h, and i by means of a Tracor/Noran spectrometer Voyager IIa, attached to a transmission electron microscope (TEM) Philips CM20FEG, in Dresden. For that, pieces of the film were scraped from the substrate with a steel knife, and placed on a carbon-film-coated copper microscope grid. Moreover, for sample j, the Witwatersrand EDX result was checked by an RBS analysis performed in Faure, South Africa, within Ref. [55].

The results of these analyses are presented in Table III. It illustrates the inconsistencies in the x scales which were already pointed out in Ref. [55]. Note that the Dresden EDX data underestimate our Rossendorf RBS values by roughly 5 at% Ni for sample 3 as well as for sample 6. Moreover, comparing the Dresden EDX data with the Witwatersrand EDX values [55], we conclude that the latter overestimate the Ni content, according to our RBS, by roughly 6 at% close to the MIT. This is confirmed by the comparison of South African EDX and RBS data for sample j, yielding a difference of 5.3 at%. For sample i, the EDX value of Ref. [55] might be very close to the Ni content according to our RBS scale – Table III suggests that the systematic deviation of the Dresden EDX values from our RBS data could be roughly constant. Finally, an additional check with an SiNi_2 bulk standard showed the Witwatersrand EDX to overestimate the true value by roughly 3 at% there.

We consider the RBS as likely to give the most accurate x values since this method is quantitative from first principles and does not require elemental standards [57]. This is confirmed by the good agreement of both RBS scales in Table III. In our case, the relative uncertainty of the corresponding Ni:Si ratios was estimated to be better than 2 %, so that the related absolute error of the Ni content should not exceed 0.3 at% in the MIT region. The quantitative result of the EDX analysis however is influenced by a series of effects, in particular this method needs standards and various corrections [58]. Therefore, the systematic errors can amount to several at% so that the differences between the columns of Table III are not surprising.

The x data, given in Tables I to III, and discussed in the previous paragraphs, are obtained from the Ni:Si ratio ignoring all kinds of contamination. Different kinds of analysis showed oxygen contamination to be the most relevant one. By means of EDX, we obtained 4.4 and 11 at% as oxygen concentration in the samples 3 and h, respectively. If the oxygen

were distributed homogeneously in the films, a Ni concentration of 20 at% determined from the Ni:Si ratio would correspond to true 19.2 and 18 at% Ni for series A and B, respectively. However, some of the oxygen is expected to be concentrated close to the film surface and the film-substrate interface, so that this quantitative information should not be overvalued.

Both sets of films were found to be well homogeneous. Laterally we checked this by EDX and electrical measurements for both sets. Changes in vertical direction might be critical in both technologies. We used GDOES to clarify this point. Because of the non-conducting substrate, we applied our self-developed radiofrequency equipment, a new and very suitable device for studying vertical concentration variations [59]. For series B, the vertical homogeneity was also checked by monitoring the quotient of the Ni and Si evaporation rates during film deposition [55].

By means of GDOES, the Ni:Si ratio was found to deviate from the respective mean values through the thickness of the samples by not more than 5 % for both sample sets, corresponding to ± 0.7 at% Ni close to the MIT. Fig. 2 shows depth profiles for series A and B. Note the constancy of the Ni signal. The variation of the Si signal at the beginning is an artifact. It arises from the strong dependence of the intensity of the Si line used on the changing plasma parameters at ignition. This variation is caused by surface contamination indicated by the C (carbon) signal; this was checked by additional experiments. Therefore, we estimated the relative variation of the Ni:Si ratio from the Ni signal.

B. Structure

The microstructure of the samples of both sets was investigated by TEM. In all cases, the samples were found to be well amorphous. However, the existence of crystalline regions with diameters below 2 nm cannot be excluded. Such a clustering is suggested by [51], cf. [60].

The topography of the $a\text{-Si}_{1-x}\text{Ni}_x$ films was studied ex situ by means of a scanning tunneling microscope (STM) under UHV conditions ($p < 1 \cdot 10^{-9}$ mbar). For that purpose, we used a modified Omicron-UHV-STM with etched tungsten tip and partly self-made electronics. A typical topography of sample 3 is given in Fig. 3. Three corresponding cross-sections are presented in Fig. 4. For sample f, we obtained very similar results.

Figs. 3 and 4 show that there are fluctuations in the film thickness of typically ± 2 nm. In rare cases, the fluctuations reach an altitude of ± 7 nm. The horizontal diameter of these hills amounts to the order of 30 nm. However, there is also a fine structure on a smaller scale, which fact might be related to some fractal structuring [61]. Unfortunately, we have no information to what extent these structures can be considered as representing a surface roughness only, or whether they originate from a columnar film growth, see e.g. Ref. [62].

The surface roughness could cause differences between technologies A and B concerning the chemical homogeneity of the films when considering a mesoscopic length scale: The local chemical composition is independent of the surface slope in technology A. However, during gradient film deposition by means of technology B, the variation of the surface slope causes a fluctuation of the Si and Ni incidence angles, where an increase of the former is correlated with a decrease of the latter. Thus the chemical composition of these films ought to fluctuate on a mesoscopic length scale [63].

To estimate quantitatively this effect is difficult for two reasons: (i) The fluctuation strength depends on the size of the surface area taken into account in averaging. (ii) We have no information on surface and volume diffusion lengths limiting composition fluctuations. As an example, we consider a cube with edge length 2.4 nm, and assume the diffusion lengths not to exceed this value. The typical surface slope, estimated as root mean square of the difference quotient $\Delta z/\Delta x$ (with $\Delta x = 2.4$ nm) for several cross sections, corresponds to an angle of 14 degrees. For sample f, the incidence angles of the Si and Ni atoms, arriving from opposite sides, are roughly 10 and 45 degrees. This sample has a mean Ni content of 24.8 at% according to the EDX scale of Ref. [55]. Thus the fluctuation of the incidence angle due to the surface roughness causes composition fluctuations with a mean deviation of ± 6 at% Ni. This value is by a factor of 3 larger than the finite size induced random dispersion of the Ni content. However, since the regions of maximum and minimum Ni content do not form a percolative network, they have to be considered as local inclusions.

IV. CONDUCTIVITY MEASUREMENTS

Three types of measurements have been performed to study the T dependence of σ :

- (a) 2 – 300 K using a self-built cryostat insert based on a bell technique, which permits very accurate stabilization of T over the whole interval, so that a high accuracy of the values of the logarithmic derivative is guaranteed,
- (b) 0.45 – 4.2 K using an RMC ^3He cryostat, and
- (c) 35 – 900 mK using a dilution refrigerator Kelvinox 300 from Oxford Instruments.

Measurements (a) of the B samples are repetitions with increased accuracy of the investigations in Refs. [55,56]. Some of the measurements (b) were already published in Refs. [55,56]. However, within this study they were re-analyzed, and the values of the logarithmic derivative were re-calculated by means of Eqs. (8,9) below.

Two methods of making contacts to the samples were used: The leads were attached either by pressing indium tabs onto the sample, or by silver paste. Both these technologies avoid post-preparation heating of the films, but they need care to avoid contact problems in thermal cycling.

A specific problem consists in the aging of the samples which can cause a resistivity change up to the order of 10 %. Thus we performed annealing experiments: Metallic films are influenced only slightly by annealing below roughly 150°C, but annealing up to about 300°C leads to great changes, cf. Refs. [48,49]. Repeated thermal cycling between cryogenic and room temperatures can cause resistivity changes by a few % as well, but no drift is detectable in thermal cycling between 2 and 4.2 K. The usual aging concerns only the absolute value of the resistivity; the resistivity ratio $R(T)/R(300\text{ K})$ was observed to remain almost unchanged. Therefore we do not consider the sample after aging / thermal cycling to be a different sample, as if prepared under different conditions, and we simply scale the resistivity when necessary to retain the original value at an appropriate T . However, this scaling is irrelevant for the consideration of the logarithmic derivative, on which the main conclusion of this paper is based.

Overviews for both the data sets A and B are shown in Fig. 5. Both data sets exhibit consistent behavior, with some systematic differences between them. For comparison, Fig. 5a includes data of two sputtered $\text{a-Si}_{1-x}\text{Ni}_x$ films from Ref. [50], resembling the curves

of our evaporated samples very much. However, it is almost impossible to obtain reliable information on physical mechanisms directly from these only weakly structured curves.

V. CONDUCTIVITY DATA ANALYSIS

A. Standard extrapolation

The standard analysis for determining the critical concentration of the MIT, based on extrapolation according to Eq. (2) with $p = 1/2$, is presented in Fig. 6. Indeed, if only data points between roughly 2 and 30 K are taken into consideration, linear relations corresponding to Eq. (2) are found in the σ versus $T^{1/2}$ representations. According to this analysis the MIT should be located just below the x of sample 1 in set A, and between samples c and d in set B. However, inclusion of the data around and below about 1 K shows that this classification is questionable.

B. The logarithmic derivative

More insight can be gained by considering the logarithmic derivative,

$$w(T) = \frac{d \ln \sigma(T)}{d \ln T} . \quad (3)$$

Its limiting behavior for vanishing T allows one to detect the transition point [19].

As a first approach to an understanding of how $w(T, x)$ reflects the character of the MIT, let us assume that, for a given sample, the logarithmic derivative of the conductivity can be approximated by

$$w(T) = c + d \cdot (T/T_m)^q , \quad (4)$$

where T_m is an experimentally accessible temperature, at which σ has been measured.

Integration of Eq. (4) yields for $q \neq 0$:

$$\ln \sigma(T_m) - \ln \sigma(T) = c \cdot (\ln T_m - \ln T) + d \cdot [1 - (T/T_m)^q]/q , \quad (5)$$

so that

$$\sigma(T) = \sigma(T_m) \cdot (T/T_m)^c \cdot \exp\{-d[1 - (T/T_m)^q]/q\} . \quad (6)$$

For $q = 0$, we can assume $d = 0$, and get from Eq. (4):

$$\sigma(T) = \sigma(T_m) \cdot (T/T_m)^c . \quad (7)$$

Interpreting Eqs. (6,7), we have to discriminate between the eight situations listed in Table IV. According to this table, $w(T \rightarrow 0) = 0$ indicates metallic character of the conduction, whereas both diverging and finite positive $w(T \rightarrow 0)$ point out that the sample is an insulator, cf. Refs. [19–22,64]. In more detail, diverging and finite positive $w(T \rightarrow 0)$ are correlated with vanishing of σ as $T \rightarrow 0$ according to exponential and power laws, respectively, cf. Eqs.

(6,7). Studying an MIT, we can exclude the case that the limit $w(T \rightarrow 0) < 0$, corresponding to $\sigma(T \rightarrow 0) = \infty$, as unphysical. However, this does of course not exclude negative w at finite T , which can arise from weak antilocalization, or e.g. from electron-phonon scattering in good metals.

In this context, we may ask what the condition is for observing exponential behavior, $\sigma(T) \propto \exp\{-(T_0/T)^q\}$. The condition $T < T_0$ implies $w > q$. Thus there exists a low- w range where, though increase of w with decreasing T would rule out metallic conduction, it would still not be possible to identify activated conduction by detecting exponential $\sigma(T)$. However, assuming only monotonicity of w as $T \rightarrow 0$, one reaches an unambiguous decision.

The logarithmic derivative is also helpful in identifying the physical mechanisms involved [29,30,65] since it makes characteristic features of $\sigma(T)$ visible, which are not obvious from $\sigma(T)$ itself. An additional advantage of this quantity is that it is not influenced by geometrical errors, nor by the scaling of the resistivity mentioned above.

Our method of data evaluation for analyses in terms of w is based on that used in Ref. [66]: A linear fit of $\ln \sigma$ versus $\ln T$ for k neighboring points is performed,

$$w_{\text{lf}} = \frac{k \sum_i \ln \sigma_i \ln T_i - \sum_i \ln \sigma_i \sum_j \ln T_j}{k \sum_i (\ln T_i)^2 - (\sum_i \ln T_i)^2}. \quad (8)$$

In order to minimize the numerical error arising from the non-linearity of the dependence of $\ln \sigma$ from $\ln T$, we relate this w value to a mean temperature, T_{lf} , defined by

$$\ln T_{\text{lf}} = \frac{k \sum_i (\ln T_i)^3 - \sum_i \ln T_i \sum_j (\ln T_j)^2}{2(k \sum_i (\ln T_i)^2 - (\sum_i \ln T_i)^2)}. \quad (9)$$

Thus w_{lf} would exactly equal $w(T_{\text{lf}})$ if $\ln \sigma$ were a second order polynomial of $\ln T$. Utilizing Eqs. (8,9) allows one to take into consideration rather broad T intervals, so that the total error (numerical plus random) can be kept small.

The optimum value of k depends on the accuracy and density of the data points, as well as on the structure of the measured curve. We considered the following groups of neighboring data points: The measurements in the region 2 – 300 K yielded data points with comparably high accuracy, but low density. From them, the logarithmic derivative was obtained using $k = 3$ below 7 K, and $k = 2$ above. In the ^3He region, the density of data points is considerably higher, thus 8 neighboring data points were considered in differentiating for all samples except for h, for which we used 4 points. The data obtained in the dilution refrigerator were evaluated using $k = 5$.

Fig. 7 gives a survey of the T dependences of the logarithmic derivative. Low- T details become visible in Fig. 8. These figures show that both the sample sets A and B are internally consistent. However, there are also significant differences between these sets.

C. Common features of the two series

Consider first the common features: For both data sets, at sufficiently high T , all samples studied behave very similarly: $w(T)$ increases with increasing T . On the other hand, for the samples with the smallest Ni content, at low T , there is a pronounced increase of $w(T)$ with decreasing T , indicating activated conduction. The strength of this contribution decreases

with increasing x . One common feature of all samples (with $w > 0$), which exhibit such an increase of w with decreasing T , has to be stressed: this increase continues down to the lowest accessible T . The extrapolation / generalization of this finding will be a basic assumption of our data analysis.

The differing behavior at low and high T must be caused by two different mechanisms being dominant at low and high T , respectively. The low- T mechanism related to increasing $w(T)$ as T decreases is very likely a kind of hopping conduction, cf. Refs. [29,30,56,65]. Concerning the origin of the high- T contribution we can only speculate. Such a high- T contribution is common to many amorphous transition-metal semiconductor alloys [8]. Comparing energy scales, it was speculated that in a-Si_{1-x}Cr_x this mechanism might be related to electron-phonon interaction [30].

The feature, which we consider to be particularly interesting in Figs. 7 and 8, is the minimum of $w(T)$ related to the crossover between these two mechanisms. This minimum is located at $T_{\min} = 150$ K for sample a, which is the most insulating sample studied. The related minimum value of w is $w_{\min} = 0.68$. The minimum shifts to lower T with increasing Ni content. This behavior has to be expected since the characteristic hopping energy should tend to 0 as the transition is approached, so that hopping only becomes dominant at lower and lower T .

Simultaneously with T_{\min} , w_{\min} decreases: For the A samples 1 and 2, $T_{\min} = 6$ K and 4 K, respectively, where $w_{\min} = 0.42$ and 0.32. For the B samples d and e, $T_{\min} = 0.8$ K and 0.2 K, respectively, where $w_{\min} = 0.15$ and 0.06.

The four samples 1, 2, d, and e must be insulating because, for them, $w(T)$ increases with decreasing T at the low- T end of the T range considered. This increase cannot be understood in terms of metallic behavior according to Eq. (2). Moreover, because of the overall behavior of $w(T, x)$ (see first paragraph of this subsection), it is very likely that this trend continues as $T \rightarrow 0$ what indicates insulating character according to Tab. IV. Furthermore, even if $w(T)$ does not increase as $T \rightarrow 0$ but only remains constant, i.e., $w(T < T_{\min}) = w_{\min}$, the samples still have to be classified as insulating, because $\sigma(T < T_{\min}) \propto T^{w_{\min}}$, cf. previous subsection. This finding rules out the classification of these four samples as metallic according to the standard procedure used in Fig. 6.

However, for the samples 3, 4, and 5, $w(T)$ seems to tend to 0 as $T \rightarrow 0$, as well as for the samples g and h. (In this judgement, we presume that, since we study an MIT, the limit $w(T \rightarrow 0) \geq 0$, see previous subsection.) For sample f, we cannot decide whether or not $w(T \rightarrow 0) = 0$ although we investigated it down to 35 mK. Thus we conclude that the MIT should take place between samples 2 and 3 for set A, and between samples e and g for set B.

In the calculation of the critical Ni contents, and of their possible errors, we take into account the Ni concentrations of the samples bracketing the transition, the uncertainty of the x values, and the influence of preparation conditions differing slightly from sample to sample in technology A. For sample sets A and B, we obtain 16.6 ± 1 at% according to our RBS scale, and 25 ± 2 at% according to the EDX scale of Ref. [55], respectively. In order to compare both values, we scale the EDX data by means of Table III: Presuming a linear relation between both EDX scales close to x_c , and the RBS value to exceed the EDX value of this study by 5 at%, one obtains 19 ± 3 at% as the critical Ni content of sample set B according to our RBS scale. Additionally performing the correction concerning the oxygen

concentration, see Section III, we obtain similar values for the critical concentration: 15.9 ± 1 and 17 ± 3 at% Ni for series A and B, respectively. Note however, that this agreement is not a necessity. On the contrary, since O is very reactive, it would not be surprising if the O contamination significantly influenced the gap states and shifted x_c , cf. the role of H in a-Si based alloys [67].

The consideration of the samples bracketing the transition in both sets shows that, at high T , samples with x just below and above x_c exhibit very similar T dependences of w – there is no experimental indication of a discontinuity in the x dependence at finite T . Hence the respective substantial variations of σ with T on both sides of the MIT must originate from the same physical mechanism, which, crudely speaking, “survives” the transition. This high- T mechanism yields a substantial contribution to w down to the lowest T studied, compare the samples closest to the MIT. Thus there is a superposition of the low- and high- T contributions, whatever mechanisms they represent, in the whole T interval investigated. This has an important consequence: In fitting simply to a pure hopping relation close to the MIT, or to Eq. (2), one might obtain a precise mathematical description, but the derived parameters would not have physical relevance.

Concerning the high- T mechanism, the comparison with a-Si_{1-x}Cr_x given in Fig. 9 is interesting. For both the a-Si_{1-x}Cr_x sample δ and the a-Si_{1-x}Ni_x sample 4, $w(300\text{ K}) \approx 0.5$. However, with decreasing T , the influence of the high- T mechanism decreases considerably faster in sample δ than in sample 4: $w(30\text{ K}) = 0.04$ and 0.16 for samples δ and 4, respectively. This faster decrease of the influence of the high- T mechanism is a general feature of a-Si_{1-x}Cr_x. It has two consequences: (i) Comparing insulating samples of both substances with the same w_{\min} , the minimum is reached in a-Si_{1-x}Cr_x at clearly higher T than in a-Si_{1-x}Ni_x, compare sample γ with sample 2 in Figs. 9 and 7a, respectively. (ii) In a-Si_{1-x}Cr_x, there are minima in $\sigma(T)$, i.e., zeros in $w(T)$, at significantly higher T than in a-Si_{1-x}Ni_x, consider samples δ and ε , and see next subsection. Thus, in contrast to a-Si_{1-x}Ni_x, there is a broad, easily accessible low- T region in a-Si_{1-x}Cr_x, where one can ignore this high- T contribution, and study the pure low- T mechanisms.

D. Differences between the two series

Besides the common features described above, there are significant differences between the data sets A and B. These differences concern both the high- T and the low- T regions.

Comparing A and B samples with similar low-temperature $w(T)$ values, the A samples are found to exhibit larger high-temperature w values, i.e., they are more strongly T dependent. In detail, $w(300\text{ K}, x_c) = 0.67 \pm 0.06$ and 0.48 ± 0.06 for sets A and B, respectively. This might indicate a similarity to a-Si_{1-x}Cr_x, where the high- T mechanism seems to lose its influence with increasing oxygen content of the films, compare Fig. 2 of Ref. [68] with Fig. 1 of Ref. [30]. The same seems to be valid for a-Si_{1-x}Ni_x: The high- T contribution has smaller influence for series B, for which the oxygen contamination is larger, as observed by EDX.

For samples exhibiting a decrease of $w(T)$ as $T \rightarrow 0$, this decrease is steeper for the A than for the B samples. Sample 3 even exhibits a zero of $w(T)$ at about 0.9 K, and for sample 4 a zero just below the lowest measuring T is very likely. But such a zero was not found for the B samples within the T region studied.

Thus, in comparing the metallic samples of both sets, i.e., 3, 4, 5 and g, h, it is puzzling that for the A but not for the B samples there is visible a contribution to $\sigma(T)$ with negative T derivative. Under what conditions such a contribution exists is a question of current interest [69]. E.g. such contributions were observed in a-Si_{1-x}Cr_x [30], as well as in heavily doped crystalline Si:P [70] and Ge:Sb [71]. It remains an open question whether the missing of this contribution in the B samples is real, or whether this contribution is obscured in set B by the low- T part of the high- T contribution. The latter hypothesis is suggested by the comparison in Fig. 7a which demonstrates that this low- T part is considerably larger in the B samples than in the A samples.

Because our experimental data on the contribution with negative $d\sigma/dT$ are very sparse, we can only speculate on the physical mechanism behind. It is likely that its origin is the same as in a-Si_{1-x}Cr_x [30,32], see also Fig. 9, heavily doped crystalline Si:P [70], and Ge:Sb [71], that means probably some interplay of electron-electron interaction and disorder. However, the interpretation in terms of precursors of a metal-superconductor transition as in a-Si_{1-x}Au_x, where both the pure constituents do not become superconducting [35], cannot be ruled out yet. Further investigations at lower T are desirable.

Since great care was taken for both sample sets concerning homogeneity, we ascribe the differences stressed to the influence of differing preparation conditions. Significant contamination by crucible material could be excluded for both sample sets: In a related GDOES study, the contamination of an A sample by copper from the crucible was found to be below 500 ppm. Concerning a crucible-material-contamination check for the B samples see Ref. [55]. Thus only three possibilities seem to remain:

- Contamination by any constituents from the residual gas,
- differing surface diffusion during deposition arising from the differences in rate and / or temperature, and
- concentration fluctuations on a mesoscopic length scale arising in the technology B, cf. Section III.

Further investigations are needed to clarify this point.

VI. DISCUSSION: THE QUALITATIVE CHARACTER OF THE MIT

A. Missing plateau in $w(T)$

The common features of both sample sets suggest an important qualitative conclusion concerning the character of the MIT, as will be explained in this section. Figs. 7 and 8, together with Tables I and II, show that $w(T = \text{const.}, x)$ decreases monotonically with increasing x , at least as long as $w > 0$. Thus there must be a separatrix (separating line), above which insulating and below which metallic samples are located in these graphs. More accurately, instead of a separatrix, there could also exist a separating strip, but this would imply a discontinuity in $\sigma(T = \text{const.}, x)$ for which there is no experimental evidence in this experiment, nor in the literature.

Now we compare the consequences of the common assumptions with experiment. For that we assume that the transition is continuous, as described by Eq. (1), and that, sufficiently close to the transition, below some temperature T^* , Eq. (2) holds. These equations imply three conclusions on $w(T, x)$:

(i) $w(T, x_c) = p$ since $a(x_c) = 0$. Thus the separatrix should be parallel to the T axis below T^* .

(ii) For metallic samples close to the MIT, $w \approx p$ as long as $a(x) \ll b(x) \cdot T^p$. In other words, since $a(x)$ vanishes as $x \rightarrow x_c$, the logarithmic derivative $w(T, x = \text{const.})$ should exhibit a plateau below T^* , which extends to lower T the closer x to x_c .

(iii) A plateau should also be present on the insulating side close to x_c below T^* for the following reasons. Since the characteristic hopping energy very likely tends continuously to 0 as $x \rightarrow x_c$, the crossover temperature, below which the influence of hopping dominates the T dependence of w , vanishes too. Continuity of $\sigma(T = \text{const.}, x)$ leads to the expectation that $w \approx \text{const.}$ above that crossover temperature.

However, according to our experimental data, such a plateau is missing. Instead, for arbitrary fixed T , $w(T, x_c)$ must be smaller than $w(T)$ of samples 2 and e, but exceed $w(T)$ of samples 3 and g for sample sets A and B, respectively. Thus, $w(T, x_c)$ decreases with decreasing T , at least down to 0.2 K, where $w(T, x_c) < 0.06$. There is no experimental hint for $w(T, x_c)$ at even lower T to rise again up to one of the theory values 1/2 or 1/3, and to saturate there; for x close to x_c , such a behavior would imply the existence of metallic $w(T)$ curves with a low- T maximum, so that it would contradict the assumption on monotonicity of $w(T)$ as T vanishes for samples with $w > 0$ and $dw/dT < 0$, concluded in Section V.C from our experimental data. Hence, at least one of the standard descriptions Eqs. (1,2) is very likely not valid: Either the relevant mechanism at the transition is related to a value of p which is far smaller than expected, or the transition is not continuous at $T = 0$, since $w(T \rightarrow 0, x_c) = 0$ indicates finite $\sigma(T \rightarrow 0, x_c + 0)$ according to Table IV.

B. Two simple models

To illustrate the problem from a different perspective, we study $w(T, x)$ for two qualitative empirical models. They are constructed so that continuity at x_c for arbitrary finite T and monotonic behavior of $\sigma(T = \text{const.}, x)$ are guaranteed.

First we assume the transition to be continuous also at $T = 0$. One of the simplest suitable models is

$$\sigma(T, x) = \begin{cases} T^{1/2} \exp\{-(T_0(x)/T)^{1/2}\} & \text{for } x < x_c \\ a(x) + T^{1/2} & \text{for } x \geq x_c \end{cases}, \quad (10)$$

where $T_0(x \rightarrow x_c - 0) = 0$, and $a(x \rightarrow x_c + 0) = 0$. For simplicity, all quantities are given in dimensionless form.

Corresponding $w(T)$ curves are presented in Fig. 10. Note that there are no pieces with $w < p = 1/2$ which belong to insulating samples, and that, if $w < p$, dw/dT is always positive.

Next we assume the transition to be discontinuous, but only at $T = 0$. We consider again a very simple qualitative model:

$$\sigma(T, x) = \begin{cases} (1 + T^{1/2}) \exp\{-(T_0(x)/T)^{1/2}\} & \text{for } x < x_c \\ a(x) + T^{1/2} & \text{for } x \geq x_c \end{cases}, \quad (11)$$

where $T_0(x \rightarrow x_c - 0) = 0$, and $a(x \rightarrow x_c + 0) = 1$. In order to illustrate how this model unifies a discontinuity of $\sigma(T = \text{const.}, x)$ at $T = 0$ with continuity for $T > 0$, we present

$\sigma(T, x = \text{const.})$ and $\sigma(T = \text{const.}, x)$ in Figs. 11a and 11b, respectively. The latter graph is based on the following additional assumptions: $x_c = 0.5$, $T_0(x) = 30 \cdot (x_c - x)^2$, and $a(x) = 1 + 3 \cdot (x - x_c)$, where using 2 as critical exponent of T_0 is motivated by [65]; however, the qualitative properties of the model considered do not depend on the numbers chosen. Figs. 11a and 11b demonstrate two remarkable features of the model (11): (i) If some low- T range, e.g. the shaded area, is masked, a misinterpretation of the activated curves closest to the MIT as metallic ones is tempting, and one could even conclude that the transition is continuous. (ii) The singularity of $\sigma(0, x)$ at x_c evolves with decreasing T because $\sigma(T = \text{const.}, x)$ becomes increasingly steep just below x_c .

Fig. 12 shows the $w(T)$ curves for model (11). Contrary to Fig. 10, this figure includes minima of $w(T, x = \text{const.})$ with very small values of $w_{\min}(x)$ at $T_{\min}(x)$, where $T_{\min}(x)$ as well as $w_{\min}(x)$ vanish as $x \rightarrow x_c$. The specific point is that $\sigma(0, x_c - 0)$ equals $\sigma(0, x_c)$ for model (10), but not for (11). In both cases, $w(0, x_c - 0) = \infty$, and $w(0, x_c + 0) = 0$; the limit $w(T \rightarrow 0, x_c)$ equals $1/2$ for model (10) and 0 for model (11).

Concerning the existence of minima in $w(T, x = \text{const.})$, Fig. 12 resembles far more the experimental figures than Fig. 10. Thus, a discontinuity of $\sigma(0, x)$ is suggested, provided $w(T, x_c)$ does not finally saturate (at some value far lower than theoretically expected) below the lowest experimentally accessible T as T decreases. However, this result was obtained using a very simple model. The question of its general validity is considered in the next subsection.

C. Mathematical view

The argumentation leading from the discontinuous character of the MIT, as modeled by Eq. (11), to the qualitative character of $w(T, x)$ shown in Fig. 12 can easily be reversed: Figs. 7 and 8 suggest the assumption that $w(T, x_c) \rightarrow 0$ as $T \rightarrow 0$. Moreover, we only need the experimentally demonstrated monotonicity of $\sigma(T = \text{const.}, x)$, that is $d\sigma/dx > 0$. We suppose it to be valid down to arbitrarily low T .

Formulated in mathematical language, Figs. 7 and 8, together with Table IV, suggest that the samples can be discriminated according to the behavior of $w(T, x)$ for vanishing T to belong to either of two groups with $x < x_c$ and $x \geq x_c$, respectively:

(i) For samples with “activated” conduction, classified as “insulating”, there is a positive $w_1(x)$, such that

$$w(T, x) \geq w_1(x) \quad \text{for all } T < T_m, \quad (12)$$

where T_m is some experimentally accessible temperature.

(ii) For “metallic” samples, there are numbers w_0 and q (independent of x) such that

$$w(T, x) \leq w_0 \cdot (T/T_m)^q \quad \text{for all } T < T_m. \quad (13)$$

We assume that we have determined $\sigma(T_m, x)$ experimentally. For the “insulating” x region, integration of Eq. (12) leads to

$$\sigma(T, x) \leq \sigma(T_m, x) \cdot (T/T_m)^{w_1(x)}, \quad (14)$$

so that

$$\sigma(0, x) = 0 \quad \text{for all } x < x_c. \quad (15)$$

Now we turn to the “metallic” region. For $x = x_c$, integration of Eq. (13) yields

$$\ln \sigma(T_m, x_c) - \ln \sigma(T, x_c) \leq w_0 \cdot [1 - (T/T_m)^q]/q, \quad (16)$$

so that

$$\sigma(0, x_c) \geq \sigma(T_m, x_c) \cdot \exp(-w_0/q) > 0. \quad (17)$$

That means $\sigma(0, x_c)$ must be finite. (In our case, Fig. 8 leads to the estimates $w_0 = 0.05$ and $q = 1/2$ for $T_m = 1$ K, so that $\exp\{-w_0/q\} \approx 0.9$.) Finally, due to the monotonicity of $\sigma(T = \text{const.}, x)$, we get

$$\sigma(0, x) > \sigma(T_m, x_c) \cdot \exp(-w_0/q) \quad \text{for all } x > x_c. \quad (18)$$

Hence, the classifications of the samples according to $w(T \rightarrow 0, x)$ and $\sigma(T \rightarrow 0, x)$, respectively, are identical, and we arrive at the following conclusion: Provided our qualitative assumptions on the limiting behavior of $w(T, x_c)$ and the monotonicity of $\sigma(T = \text{const.}, x)$ are justified, there must be a finite minimum metallic conductivity.

D. Consideration of counterarguments

We must, however, look back at our arguments to see what would be necessary for the transition nevertheless to be continuous, in which manner condition (13) would have to be weakened. Two possibilities have already been mentioned: (i) The behavior of $w(T, x)$ might qualitatively change at temperatures below the lowest one accessible to us. (ii) At x_c , the parameter c of Eq. (4) might have a small but finite value, far smaller than the values $1/2$ and $1/3$, which were predicted theoretically in Refs. [27,28] and used in many experimental studies in the literature.

A third possibility is found when referring to Eq. (5), which, for $c = 0$, simplifies to $\ln \sigma(T = 0) = \ln \sigma(T_m) - d/q$. For no discontinuity to occur, it has to be possible to reach any (arbitrarily small) $\sigma(0, x_c + 0)$. The first term, $\ln \sigma(T_m)$, is finite due to the monotonicity of $\sigma(T_m, x)$ and the finite σ values observed in the insulating region at T_m . Thus for no discontinuity to occur, d/q has to be infinite. Since $d = w(T_m)$, the exponent q must be infinitely small. For T independent q , this situation is equivalent to the case (ii) above, that is the situation of a small but finite c . The only remaining possibility is that of a T dependent q , vanishing as $T \rightarrow 0$ for $x = x_c$. This would imply a non-power law behavior of $\sigma(T, x_c)$. If one would nevertheless try to fit $\sigma \propto T^p$, the effective exponent p would be T dependent, and approach 0 as $T \rightarrow 0$.

However, we know of no physical argument that suggests that the power law (which is derived by perturbation arguments) should weaken at low T , and we did not obtain any data that suggest that there is a tendency towards such a change at lowest accessible T . Therefore, for $T = 0$, although continuity across the transition is theoretically possible, experimental evidence appears to indicate that the transition is, in fact, discontinuous.

Finally, the question remains whether or not this result might be an artifact arising from any sample inhomogeneities. We utilized all available experimental possibilities to control

and to minimize macroscopic inhomogeneities. Nevertheless, surely some small composition gradients remain. Calculating the $T = 0$ conductance of samples with constant x gradients perpendicular and parallel to the current direction, respectively, assuming Eq. (1) to be valid, one obtains the following results: In the former case, the transition is “smeared out”, but in the latter case, provided the exponent ν in Eq. (1) satisfies $0 < \nu < 1$, a sharp transition would result. However, according to the preparation technologies used, the inhomogeneities should be considerably smaller parallel to the current direction than perpendicular to it. Thus the influence of a parallel x gradient is probably overcompensated by the perpendicular inhomogeneities. Moreover, the hypothesis that the discontinuous transition for $T = 0$ might be only an artifact originating from a parallel gradient, is ruled out by the behavior of $w(T, x = \text{const.})$ for the region where $a(x) \ll b(x) \cdot T^p$. The logarithmic derivative would have to exhibit a plateau $w(T, x_c) \approx p$ here according to the gradient hypothesis, but we did not find one.

E. Minimum metallic conductivity

In summary, it is very likely that $\sigma(0, x)$ exhibits a discontinuity in a-Si_{1-x}Ni_x, corresponding to Mott’s idea of a minimum metallic conductivity σ_{mm} [2], but $\sigma(T = \text{const.} > 0, x)$ should be continuous for arbitrary finite T . However, we cannot exclude the possibility that $w(T, x_c)$ changes its behavior, in particular that it saturates at some finite value, at temperatures lower than those experimentally accessible to us. This would correspond to the T exponent in Eq. (2) becoming much smaller than expected theoretically. Thus a conclusion with complete certainty is impossible.

Our experimental data only allow us to determine bounds for σ_{mm} . From the sample sets A and B we get $20 \text{ } \Omega^{-1}\text{cm}^{-1} < \sigma_{\text{mm}} < 65 \text{ } \Omega^{-1}\text{cm}^{-1}$, and $25 \text{ } \Omega^{-1}\text{cm}^{-1} < \sigma_{\text{mm}} < 70 \text{ } \Omega^{-1}\text{cm}^{-1}$, respectively. It is instructive to compare these data with Mott’s theoretical result for σ_{mm} [2,72], though electron-electron interaction and weak localization effects are neglected in its derivation. According to Ref. [72], $\sigma_{\text{mm}} = 0.026 e^2/(\hbar a)$, where a denotes the distance between neighboring impurity atoms, i.e., Ni atoms, at the MIT. Taking the atomic density of the samples to be similar that in crystalline Si, we get $a \approx 5 \text{ } \text{\AA}$. This estimate fits with the Mott-Edwards-Sienko criterion, $a_{\text{H}}^* \cdot n_c^{1/3} \approx 0.25$ with a_{H}^* being the Bohr orbit radius of an isolated center and n_c the critical impurity density [73–75]: Approximating a_{H}^* by half the nearest neighbor distance of crystalline Ni, $a_{\text{H}}^* \approx 1.24 \text{ } \text{\AA}$, yields just the expected product value. Finally, we obtain $\sigma_{\text{mm}} \approx 120 \text{ } \Omega^{-1}\text{cm}^{-1}$. This result exceeds our lower and upper bounds on σ_{mm} by factors of roughly 5 and 2, respectively. Note however that the above consideration does not take account of the possible d character of the Ni states; moreover, the dimensionless parameters have some uncertainty.

For comparison, for a-Si_{1-x}Cr_x, the conductivity studies lead to $\sigma_{\text{mm}} \approx 250 \text{ } \Omega^{-1}\text{cm}^{-1}$ [29,30]. In that substance, annealing causes a conductivity decrease [30], but the question whether or not annealing also causes a decrease of σ_{mm} is still open. However, due to the differences between the phase diagrams of the systems Si-Ni and Si-Cr, see Section I, the following hypothesis is suggested: If, instead of the Ni-Ni distance, the distance between metallic NiSi₂ grains were the relevant length for σ_{mm} , the relatively small value of σ_{mm} in a-Si_{1-x}Ni_x might result from the formation of NiSi₂ crystalline regions with a diameter of the order of 1 to 2 nm, cf. [51,60]. Corresponding structural studies would be interesting.

VII. CONCLUSIONS

The main result of our study is the following: the T dependence of the logarithmic temperature derivative of the conductivity, $w(T, x) = d \ln \sigma / d \ln T$, for $\text{a-Si}_{1-x}\text{Ni}_x$ qualitatively differs from the predictions of commonly accepted theory. According to this theory, $\sigma(0, x)$ is continuous, and, on the metallic side of the MIT, $\sigma(T, x) = a(x) + b(x) \cdot T^p$, where p should equal $1/2$ or $1/3$. Thus $w(T, x_c) = p$, and, for $w < p$, only positive dw/dT is expected. However, we observed characteristic minima of $w(T, x = \text{const.})$, where not only T_{\min} but also w_{\min} seem to tend to 0 as $x \rightarrow x_c$ from the insulating side. Below T_{\min} , w was observed to increase monotonically with decreasing T . The detailed analysis of this feature favors the discontinuous character of the MIT at $T = 0$, in the sense of Mott's original prediction of a finite minimum metallic conductivity.

The question arises why a minimum metallic conductivity was found in $\text{a-Si}_{1-x}\text{Ni}_x$, and previously in $\text{a-Si}_{1-x}\text{Cr}_x$ [29–33], but not in many of the other substances, e.g. crystalline Si:P, investigated so far. Of course, at the present stage, one cannot exclude the possibility of $\text{a-Si}_{1-x}\text{Ni}_x$ and Si:P belonging to different universality classes. Simultaneously, however, the question arises as to whether an analysis using $w(T, x)$ of previous experiments might reveal similar contradictions between standard description and experimental data as we found here. But, for the lack of sufficiently detailed information on these investigations, this question has to be postponed to future studies. Such analyses should be highly interesting since samples with $w < 1/3$ and negative dw/dT at the lowest T were also found in experiments on crystalline Si:As [76] and Si:(P,B) [21], on amorphous $\text{Si}_{1-x}\text{Cr}_x$ [77] and $\text{Si}_{1-x}\text{Mn}_x$ [78], as well as on granular Al-Ge [22]. But there is also one case in the literature, where, for such a sample, w first increases and then clearly decreases as T vanishes: the a-Cr-SiO_x sample 7 in Ref. [79] (see Fig. 2 of that work). Moreover, to the best of our knowledge, none of the experiments, which are interpreted as proof of the continuity of the MIT at $T = 0$, excludes that the “metallic” samples very close to the MIT could be insulating with a characteristic hopping temperature smaller than the lowest experimentally accessible T [18,19].

Additionally to the result concerning the character of the MIT, we consider the following points as important conclusions:

- Although both the sample sets A and B, prepared with different technologies, differ significantly concerning $\sigma(T, x)$, their critical Ni concentrations are close: 15.9 ± 1 and 17 ± 3 at%, respectively, related to our RBS scale.
- A high- T mechanism, which “survives” the transition, masks the specific localization features to a large extent in both sample sets. It remains relevant down to temperatures of several hundred mK. Thus determining theoretical parameters by fitting conductivity formulae which account only for one mechanism is not justified for $\text{a-Si}_{1-x}\text{Ni}_x$ within the considered (T, x) region.
- For $\text{a-Si}_{1-x}\text{Ni}_x$ also, it is possible to prepare metallic samples with the conductivity increasing with decreasing T . However, the influence of the mechanism from which this feature originates is weak, and it is directly visible only for certain preparation conditions.

We would also like to stress a technological consequence of our STM investigations: When evaporating from two crucibles, the surface roughness of the films is large enough to lead to substantial concentration fluctuations on a mesoscopic length scale, caused by fluctuating incidence angles. To what extent these fluctuations are washed out by diffusion is an open

question.

Finally, we turn to the question of what can be learned concerning the nature of the MIT in $\text{a-Si}_{1-x}\text{Ni}_x$ from the phenomenological results obtained above. Our findings are in disagreement with conclusions drawn from the treatment of the MIT in terms of one-parameter scaling theory [3] of Anderson localization of non-interacting electrons. But, on their own, they cannot explain why this description fails. For example, they do not tell us whether it is because electron-electron interaction had to be taken into account, nor whether two (or even more) scaling parameters would be needed to get an adequate result. Therefore, measurements of other quantities have to be consulted. XPS, UPS, and XES studies [50,54], as well as optical measurements [52,53] have shown how the gap in the density of states shrinks and finally closes with increasing Ni content, and how the Fermi energy is shifted in this process. However, for reasons of resolution, such experiments do not yield information on the important immediate vicinity of the MIT since the characteristic energy (temperature) of the hopping conduction vanishes as x approaches x_c from below.

A helpful hint comes from low- T hopping conduction deep in the insulating region [42,43] – there, it has a far stronger influence on w than the high-temperature mechanism which survives the MIT. Since the value of the hopping exponent q in the approximation $\sigma \propto \exp\{-(T_0/T)^q\}$ is close to $1/2$, and thus considerably exceeds Mott’s result $1/4$ for non-interacting electrons [80], electron-electron interaction probably is important – the question whether or not this value can be interpreted in terms of hopping in the Coulomb gap is still under controversial debate, see e.g. [81–83]. Thus, it seems likely that the MIT arises from interwoven localization and electron-electron interaction processes, cf. the speculations in Ref. [8]. A theoretical approach in this direction was very recently published by Chitra and Kotliar [84]. These authors incorporate the *long-range* Coulomb interaction into dynamical mean-field theory, and obtain the result that the MIT should be discontinuous in two- and three-dimensional systems. However, if this hypothesis is true, we would be left with a new puzzle: Why does Mott’s estimate of the minimum metallic conductivity, the derivation [72] of which neglects electron-electron interaction, still yield a reasonable value for σ_{mm} in $\text{a-Si}_{1-x}\text{Ni}_x$?

ACKNOWLEDGMENTS

This work was supported by the German-Israeli Foundation for Scientific Research and Development. We are indebted to many colleagues for helpful discussions, in particular to B. Altshuler, W. Brückner, G. Diener, A. Finkel’stein, P. Häussler, B. Kramer, C. Lauinger, Z. Ovadyahu, G. Reiss, and U. Rössler. We are much obliged to A. Isobe, M. Yamada, and K. Tanaka for sending us their $\sigma(T)$ data of sputtered films. Special thanks go to S. Geoghegan for the support in presenting three-dimensional STM data by means of Mathematica.

REFERENCES

- [1] P.W. Anderson, Phys. Rev. **109**, 1492 (1958).
- [2] N.F. Mott, Phil. Mag. **26**, 1015 (1972).
- [3] E. Abrahams, P.W. Anderson, D.C. Licciardello, and T.V. Ramakrishnan, Phys. Rev. Lett. **42**, 673 (1979).
- [4] A.M. Finkel'stein, Zh. Eksp. Teor. Fiz. **84**, 168 (1983) [Sov. Phys. JETP **57**, 97 (1983)].
- [5] A.M. Finkel'stein, Pisma Zh. Eksp. Teor. Fiz. **37**, 436 (1983) [Sov. Phys. JETP Lett. **37**, 517 (1983)].
- [6] A.M. Finkel'stein, Zh. Eksp. Teor. Fiz. **86**, 367 (1984) [Sov. Phys. JETP **59**, 212 (1984)].
- [7] P.A. Lee and T.V. Ramakrishnan, Rev. Mod. Phys. **57**, 287 (1985).
- [8] A. Möbius, J. Phys. C **18**, 4639 (1985).
- [9] N.F. Mott, *Metal-Insulator Transitions*, Second Edition (Taylor and Francis, London, 1990).
- [10] B. Kramer and A. MacKinnon, Rep. Prog. Phys. **56**, 1469 (1993).
- [11] D. Belitz and T.R. Kirkpatrick, Rev. Mod. Phys. **66**, 261 (1994).
- [12] P.P. Edwards, in *Perspectives in Solid State Chemistry*, ed. K.J. Rao, (Wiley, New York, 1995), p. 250.
- [13] M.A. Paalanen, T.F. Rosenbaum, G.A. Thomas, and R.N. Bhatt, Phys. Rev. Lett. **48**, 1284 (1982).
- [14] G.A. Thomas, M. Paalanen, and T.F. Rosenbaum, Phys. Rev. B **27**, 3897 (1983).
- [15] G. Hertel, D.J. Bishop, E.G. Spencer, J.M. Rowell, and R.C. Dynes, Phys. Rev. Lett. **50**, 743 (1983).
- [16] Peihua Dai, Youzhu Zhang, and M.P. Sarachik, Phys. Rev. Lett. **66**, 1914 (1991).
- [17] H. Stupp, M. Hornung, M. Lakner, O. Madel, and H. v. Löhneysen, Phys. Rev. Lett. **71**, 2634 (1993).
- [18] T.G. Castner, Phys. Rev. Lett. **73**, 3600 (1994).
- [19] A. Möbius, Phys. Rev. B **40**, 4194 (1989).
- [20] M.J. Hirsch, U. Thomanschefsky, and D.F. Holcomb, Phys. Rev. B **40**, 4196 (1989).
- [21] U. Thomanschefsky and D.F. Holcomb, Phys. Rev. B **45**, 13 356 (1992).
- [22] R.L. Rosenbaum, M. Slutzky, A. Möbius, and D.S. McLachlan, J. Phys.: Cond. Matt. **6**, 7977 (1994).
- [23] S.V. Kravchenko, G.V. Kravchenko, J.E. Furneaux, V.M. Pudalov, and M. D'Iorio, Phys. Rev. B **50**, 8039 (1994).
- [24] S.V. Kravchenko, Whitney E. Mason, G.E. Bowker, J.E. Furneaux, V.M. Pudalov, and M. D'Iorio, Phys. Rev. B **51**, 7038 (1995).
- [25] S.V. Kravchenko, D. Simonian, M.P. Sarachik, Whitney Mason, and J.E. Furneaux, Phys. Rev. Lett. **77**, 4938 (1996).
- [26] G.B. Lubkin, Physics Today **50**, No. 7, 19 (1997).
- [27] B.L. Altshuler and A.G. Aronov, Zh. Eksp. Teor. Fiz. **77**, 2028 (1979) [Sov. Phys. JETP **50**, 968 (1979)].
- [28] D.J. Newson and M. Pepper, J. Phys. C **19**, 3983 (1986).
- [29] A. Möbius, D. Elefant, A. Heinrich, R. Müller, J. Schumann, H. Vinzelberg, and G. Zies, J. Phys. C **16**, 6491 (1983).
- [30] A. Möbius, H. Vinzelberg, C. Gladun, A. Heinrich, D. Elefant, J. Schumann, and G. Zies, J. Phys. C **18**, 3337 (1985).

- [31] A. Möbius, phys. stat. sol. (b) **144**, 759 (1987).
- [32] A. Möbius, Z. Phys. B **79**, 265 (1990).
- [33] A. Möbius, Z. Phys. B **80**, 213 (1990).
- [34] *Binary Alloy Phase Diagrams*, ed. in chief: T.B. Massalski, second edition, (ASM International, Materials Park, 1992).
- [35] N. Nishida, M. Yamaguchi, T. Furubayashi, K. Morigaki, H. Ishimoto, and K. Ono, Solid State Commun. **44**, 305 (1982), and refs. therein.
- [36] B.W. Dodson, W.L. McMillan, J.M. Mochel, and R.C. Dynes, Phys. Rev. Lett. **46**, 46 (1981).
- [37] M. Ohring, *The Materials Science of Thin Films*, (Academic Press, Boston, 1992), p. 235.
- [38] J.O. Olowolafe, M.A. Nicolet, and J.W. Mayer, J. Appl. Phys. **47**, 5182 (1976).
- [39] E.G. Colgan, B.Y. Tsaur, and J.W. Mayer, Appl. Phys. Lett. **37**, 938 (1980).
- [40] G. Sobe and G. Zies, private communication (1984).
- [41] *Properties of Metal Silicides*, eds. K. Maex and M. van Rossum, EMIS Datareviews Series No. 14, (INSPEC, London, 1995).
- [42] K.M. Abkemeier, C.J. Adkins, R. Asal, and E.A. Davis, J. Phys.: Cond. Matt. **4**, 9113 (1992).
- [43] K.M. Abkemeier, C.J. Adkins, R. Asal, and E.A. Davis, Phil. Mag. B **65**, 675 (1992).
- [44] U. Dammer, C.J. Adkins, R. Asal, and E.A. Davis, J. Non-Cryst. Sol. **164–166**, 501 (1993).
- [45] U. Dammer, *The Metal-Insulator Transition in Amorphous Silicon-Nickel Alloys*, Master of Philosophy Thesis, University of Cambridge (1992).
- [46] M.M. Collver, Solid State Commun. **23**, 333 (1977).
- [47] M.M. Collver, Appl. Phys. Lett. **32**, 574 (1978).
- [48] C. Segal, A. Gladkikh, M. Pilosof, H. Behar, M. Witcomb, and R. Rosenbaum, J. Phys.: Condens. Matter **10**, 123 (1998).
- [49] A. Belu-Marian, M.D. Serbanescu, R. Manaila, E. Ivanov, O. Malis, A. Devenyi, Thin Solid Films **259**, 105 (1995).
- [50] A. Isobe, M. Yamada, and K. Tanaka, J. Phys. Soc. Jap. **66**, 2103 (1997).
- [51] A.M. Edwards, M.C. Fairbanks, A. Singh, R.J. Newport, and S.J. Gurman, Physica B **158**, 600 (1989).
- [52] E.A. Davis, S.C. Bayliss, R. Asal, and M. Manssor, J. Non-Cryst. Sol. **114**, 465 (1989).
- [53] R. Asal, S.C. Bayliss, and E.A. Davis, J. Non-Cryst. Sol. **137&138**, 931 (1991).
- [54] A. Gheorghiu, C. S  n  maud, R. Asal, and E.A. Davis, J. Non-Cryst. Sol. **182**, 293 (1995).
- [55] R. Rosenbaum, A. Heines, A. Palevski, M. Karpovski, A. Gladkikh, M. Pilosof, A.J. Daneshvar, M.R. Graham, T. Wright, J.T. Nicholls, C.J. Adkins, M. Witcomb, V. Prozesky, W. Przybylowicz, and R. Pretorius, J. Phys.: Condens. Matter **9**, 5395 (1997).
- [56] R. Rosenbaum, A. Heines, M. Karpovski, M. Pilosof, and M. Witcomb, J. Phys.: Condens. Matter **9**, 5413 (1997).
- [57] M. Ohring, *The Materials Science of Thin Films*, (Academic Press, Boston, 1992), p. 294.
- [58] A.P. Mackenzie, Rep. Prog. Phys. **56**, 557 (1993).

- [59] V. Hoffmann, H.-J. Uhlemann, F. Präßler, K. Wetzig, and D. Birus, *Fresenius J. Anal. Chem.* **355**, 826 (1996).
- [60] M.B. Fernandez van Raap, M.J. Regan, and A. Bienenstock, *J. Non-Cryst. Sol.* **191**, 155 (1995).
- [61] A.-L. Barabasi and H.E. Stanley, 'Fractal Concepts in Surface Growth', Cambridge University Press, 1995.
- [62] G.S. Bales and A. Zangwill, *J. Vac. Sci. Technol. A* **9**, 145 (1991).
- [63] H. van Kranenburg and C. Lodder, *Mat. Sc. and Eng.* **R11**, 295 (1994).
- [64] Jonathan R. Friedman, Youzhu Zhang, Peihua Dai, and M.P. Sarachik, *Phys. Rev. B* **53**, 9528 (1996).
- [65] A.G. Zabrodskii and K.N. Zinov'eva, *Zh. Eksp. Teor. Fiz.* **86**, 727 (1984) [*Sov. Phys. JETP* **59**, 425 (1984)].
- [66] A. Möbius, *J. Phys. C* **21**, 2789 (1988).
- [67] T. Wright, B. Popescu, C.J. Adkins, and E.A. Davis, *J. Phys.: Condens. Matter* **8**, 6737 (1996).
- [68] C. Gladun, A. Heinrich, F. Lange, J. Schumann, and H. Vinzelberg, *Thin Solid Films* **125**, 101 (1985).
- [69] A. Albers and D.S. McLachlan, *Czech. J. Phys.* **46**, Suppl. S2, 753 (1996).
- [70] T.F. Rosenbaum, K. Andres, G.A. Thomas, and P.A. Lee, *Phys. Rev. Lett.* **46**, 568 (1981).
- [71] G.A. Thomas, A. Kawabata, Y. Ootuka, S. Katsumoto, S. Kobayashi, and W. Sasaki, *Phys. Rev. B* **26**, 2113 (1982).
- [72] N.F. Mott and E.A. Davis, *Electronic Processes in Non-Crystalline Materials*, Second Edition (Clarendon, Oxford, 1979).
- [73] N.F. Mott, *Can. J. Phys.* **34**, 1356 (1956).
- [74] P.P. Edwards and M. Sienko, *Phys. Rev. B* **17**, 2575 (1978).
- [75] P.P. Edwards and M. Sienko, *Int. Rev. Phys. Chem.* **3**, 83 (1983).
- [76] W.N. Shafarman, D.W. Koon, and T.G. Castner, *Phys. Rev. B* **40**, 1216 (1989).
- [77] In Refs. [29,30], increase of w with decreasing σ is presented for $\text{Si}_{1-x}\text{Cr}_x$. Due to $d\sigma/dT > 0$, this corresponds to $dw/dT < 0$.
- [78] A.I. Yakimov, A.V. Dvurechenskii, and C.J. Adkins, *phys. stat. sol. (b)* **205**, 299 (1998).
- [79] H. Vinzelberg, A. Heinrich, C. Gladun, and D. Elefant, *Phil. Mag. B* **65**, 651 (1992).
- [80] N.F. Mott, *J. Non-Cryst. Sol.* **1**, 1 (1968).
- [81] A.L. Efros and B.I. Shklovskii, *J. Phys. C* **8**, L49 (1975).
- [82] C.J. Adkins, *J. Phys.: Condens. Matter* **1**, 1253 (1989).
- [83] M. Pollak, *phys. stat. sol. (b)* **205**, 35 (1998).
- [84] R. Chitra and G. Kotliar, *cond-mat/9903180*.

TABLES

Sample	$x/\text{at\% Ni}$	t/nm	$\sigma(300\text{ K})/\Omega^{-1}\text{cm}^{-1}$	$\sigma(4.2\text{ K})/\Omega^{-1}\text{cm}^{-1}$
1	14.9	159	150	15
2	16.4	183	160	20
3	16.7	179	245	64
4	18.9	181	340	145
5	22.1	162	585	330
6	55.9	175	—	—

TABLE I. Ni content x , film thickness t , conductivity σ at room and liquid-helium temperatures for sample set A. The x values are obtained from the Ni:Si ratio measured by RBS within this work; their uncertainty amounts to 0.3 at% for samples 1 – 5, and to 0.5 at% for sample 6.

Sample	$x/\text{at\% Ni}$	t/nm	$\sigma(300\text{ K})/\Omega^{-1}\text{cm}^{-1}$	$\sigma(4.2\text{ K})/\Omega^{-1}\text{cm}^{-1}$
a (23)	19.5	121	42	1.0
b (22)	20.3	122	54	2.7
c (21)	21.2	124	73	8.0
d (20)	22.3	124	88	18
e (19)	23.5	123	120	30
f (18)	24.8	122	160	60
g (17)	26.4	120	190	82
h (16)	28.2	118	280	160
i (8)	42.9	89	790	—
j (—)	25.3	—	—	—

TABLE II. Ni content x , film thickness t , conductivity σ at room and liquid-helium temperatures for sample set B. The sample names in parentheses are the notations used in Ref. [55,56]. Sample j, positioned between samples f and g during film deposition, was prepared specifically for EDX and RBS analyses within that work. The x values are the EDX data published in either Tab. I of those papers.

Sample	RBS-R	RBS-F	EDX-D	EDX-W
3	16.7	–	11.6	–
3	16.7	–	12.0	–
6	55.9	–	51.7	–
f	–	–	14.0	24.8
h	–	–	20.3	28.2
i	–	–	37.8	42.9
j	–	20.0	–	25.3

TABLE III. Comparison of Ni contents as determined by RBS in Rossendorf (RBS-R) and Faure (RBS-F), and by EDX in Dresden (EDX-D) and Witwatersrand (EDX-W). The RBS-R and EDX-D data were obtained within this work, whereas the RBS-F and EDX-W results are taken from Ref. [55], – unfortunately, Ref. [55] contained a mistake in evaluating x from the Si:Ni ratio obtained by RBS-F, which is corrected here. All Ni contents were obtained from the Si:Ni ratios, ignoring impurity contamination. The random error of the EDX measurement within this study does not exceed 0.5 at% Ni. The first two lines serve also as reproducibility check of EDX-D; these measurements were performed fully independently at two different days, when different pieces of the film were investigated.

q	c	d	$w(T \rightarrow 0)$	$\sigma(T \rightarrow 0)$	character
< 0	arbitrary	< 0	$-\infty$	∞	ideal metal
< 0	arbitrary	> 0	∞	0	insulator
$= 0$	< 0	$= 0$	< 0	∞	ideal metal
$= 0$	$= 0$	$= 0$	$= 0$	finite	real metal
$= 0$	> 0	$= 0$	> 0	0	insulator
> 0	< 0	arbitrary	< 0	∞	ideal metal
> 0	$= 0$	arbitrary	$= 0$	finite	real metal
> 0	> 0	arbitrary	> 0	0	insulator

TABLE IV. Behavior of $\sigma(T \rightarrow 0)$, and character of the conduction process in dependence on the parameters in Eq. (4), modelling $w(T \rightarrow 0)$. Here, “ideal metal” stands for $\sigma(T \rightarrow 0) = \infty$ (no impurity scattering). For simplicity, if $q = 0$, we assume $d = 0$; moreover, we consider $d = 0$ only for $q = 0$.

FIGURES

FIG. 1. Experimental parameter plane: The insulating region, where only activated conduction occurs, is marked by I, the metallic region by M, and the lowest experimentally accessible temperature by T_{lea} . Measuring $\sigma(T, x = \text{const.})$ means to obtain data points (\bullet , \times) along vertical lines in this graph. The characteristic hopping temperature, $T_{\text{hop}}(x)$, is marked by a full line. Only for $T < T_{\text{hop}}$, σ depends exponentially on T . For $T > T_{\text{hop}}$, comparably flat, non-exponential $\sigma(T)$ dependences are expected. Thus, for \bullet , depending on T , both exponential and non-exponential behavior are observed. However, for \times , only non-exponential $\sigma(T, x = \text{const.})$ are found, although this sample belongs to the insulating region, too. The latter problem occurs in the whole interval $[x^*, x_c)$.

FIG. 2. Glow discharge optical emission spectroscopy (GDOES) depth profiles for the elements B, C, Ni, and Si, i.e., intensity I versus sputtering time t , for two samples prepared by technologies A and B, respectively. (a) presents the analysis of sample 5, whereas (b) shows data for a sample prepared specifically for this analysis together with samples a – i; due to the simultaneous preparation, (b) is representative for the whole sample set B. We made use of the following lines: B - 208.9 nm, C - 156.1 nm, Ni - 349.2 nm, and Si - 288.1 nm. The intensity scales were adjusted to reach a high resolution, thus the units differ from element to element. In (a), the sudden increase of the B signal indicates the moment when the bottom of the sputtering crater reaches the glass substrate.

FIG. 3. STM image of the surface topography of sample 3, measured with a current of 0.5 nA and a bias of 8 V. The figure was obtained using a slope correction and a slight smoothing of the row data.

FIG. 4. Three STM cross sections of the surface of sample 3 obtained with different resolutions (current = 0.3 nA, bias = 8 V). The data presented are obtained from the row data performing only a slope correction. In all cases, the height was determined at 128 points along a line segment, slightly longer than represented.

FIG. 5. Overview of $\sigma(T, x)$ in double logarithmic representations for sets A (+) and B (\times) in graphs (a) and (b), respectively. For the characterization of the samples see Tables I and II. To illustrate common as well as differing features, both graphs include a sample of the other set, for the sake of distinctness marked by \bullet . Moreover, (a) includes data for two sputtered a-Si_{1-x}Ni_x films (\blacktriangle) from Ref. [50]. These samples, here referred to as α and β , have a Ni content of 20.7, and 27.1 at%, respectively, as determined by an EDX analysis [50].

FIG. 6. $\sigma(T, x)$ versus $T^{1/2}$ representation of the samples closest to the MIT for sets A (+) and B (\times) in graphs (a) and (b), respectively. Both graphs include one sample of the other set (\bullet). The dashed lines give the extrapolations according to Eq. (2) with $p = 1/2$, obtained from the region 2 – 30 K.

FIG. 7. Overview of the T and x dependence of the logarithmic derivative, $w = d \ln \sigma / d \ln T$ for sets A (+) and B (\times) in graphs (a) and (b), respectively. Both graphs include one curve of the other set (\bullet). The temperature scale $T^{1/2}$ is chosen in order to have reasonable resolution also for the low- T part.

FIG. 8. Low- T / low- w part of Fig. 7. The data presented were obtained from measurements in three different cryostats, see Section IV, where several months passed between the investigations. Moreover, in some cases, contacts had to be renewed between the measurements.

FIG. 9. Comparison of $w(T)$ for the a-Si $_{1-x}$ Ni $_x$ sample 4 (\bullet) with the $w(T)$ for three a-Si $_{1-x}$ Cr $_x$ samples (*), here referred to as γ , δ , and ε . The a-Si $_{1-x}$ Cr $_x$ curves were obtained from $\sigma(T)$ data, published in Figs. 1 and 7 of Ref. [30]. Samples γ , δ , and ε , have a Cr content of 11, 14, and 19 at%, respectively, obtained by EDX [30]. Calculating w , we used $k = 4$ for samples γ and ε , and $k = 2$ for δ .

FIG. 10. Qualitative behavior of $w(T, x)$ for a continuous transition according to Eq. (10). Dashed lines: insulating with $T_0(x)^{1/2} = 0.03, 0.1, 0.3$, and 1; full lines: metallic with $a(x) = 0.03, 0.1, 0.3$, and 1; dashed-dotted line: separatrix between insulating and metallic regions.

FIG. 11. Characteristic $\sigma(T, x)$ features of a discontinuous transition according to Eq. (11): T and x dependences of σ are shown in graphs (a) and (b), respectively. Dashed and full lines represent insulating and metallic regions, respectively; the dashed-dotted line in (a) denotes the separatrix between these regions. The lines shown in (a) were obtained for the parameter values $T_0(x)^{1/2} = 0.05, 0.15, 0.5, 1.5$, and $a(x) - 1 = 0.2, 0.6, 1.0, 1.4$. Shaded area in (a): example of low- T range being inaccessible in a real experiment.

FIG. 12. Qualitative behavior of $w(T, x)$ for a discontinuous transition according to Eq. (11). Dashed lines: insulating with $T_0(x)^{1/2} = 0.02, 0.06, 0.2$, and 0.6; full lines: metallic with $a(x) - 1 = 0.2, 0.6, 2$, and 6; dashed-dotted line: separatrix between insulating and metallic regions.

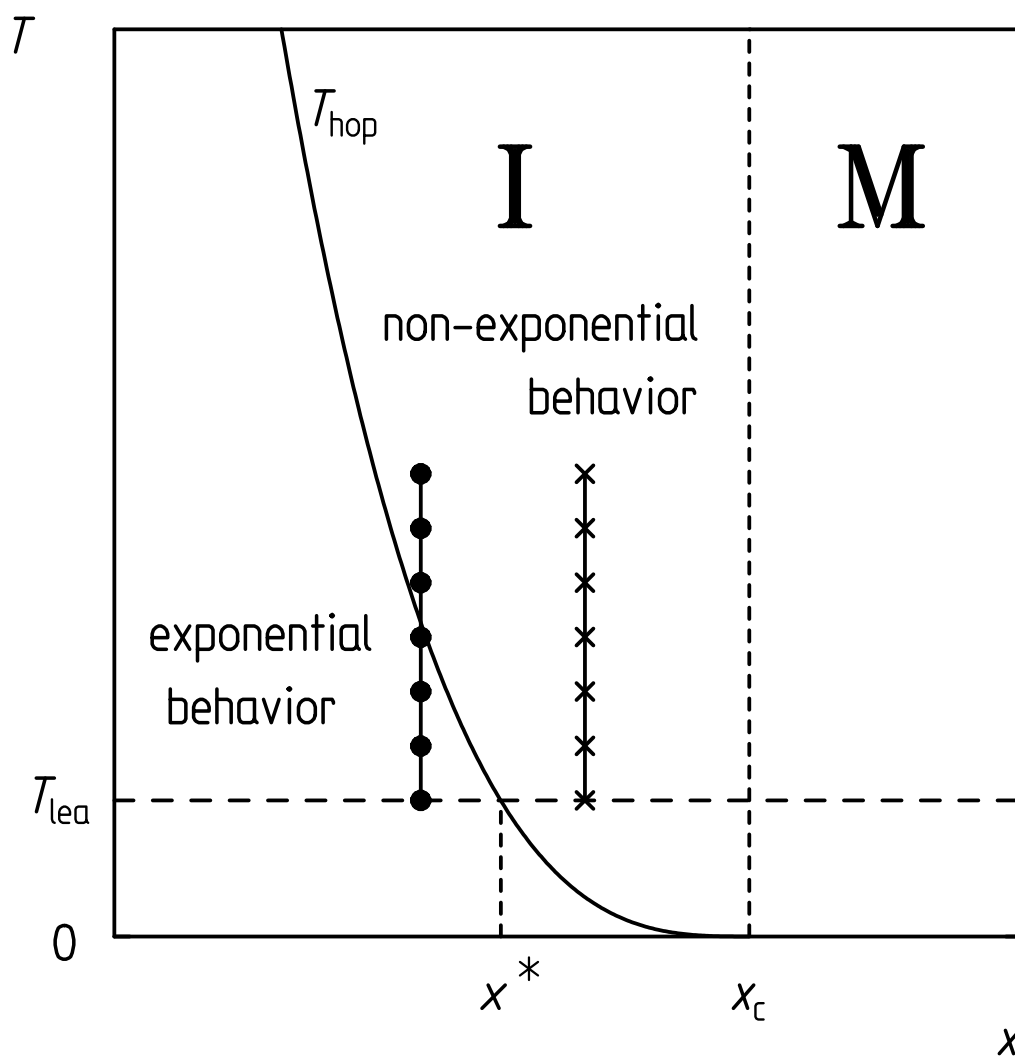


Fig. 1

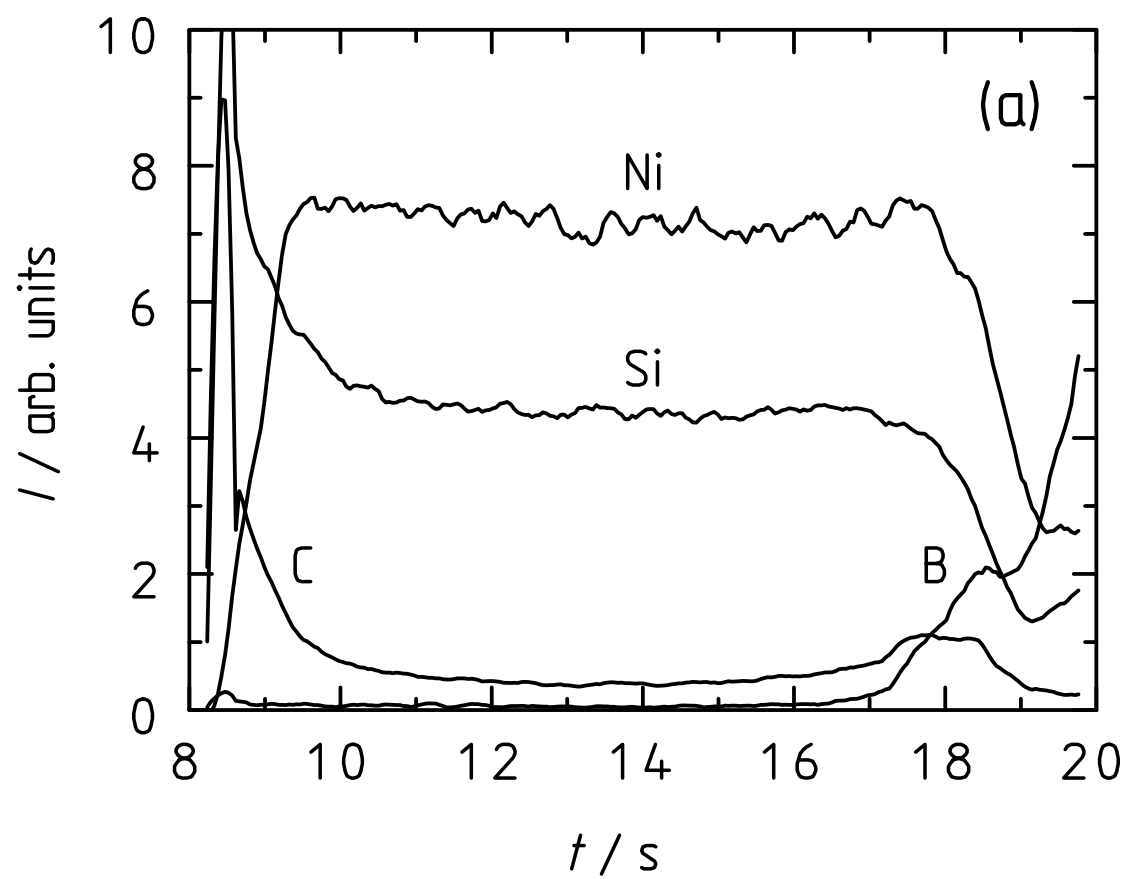


Fig. 2a

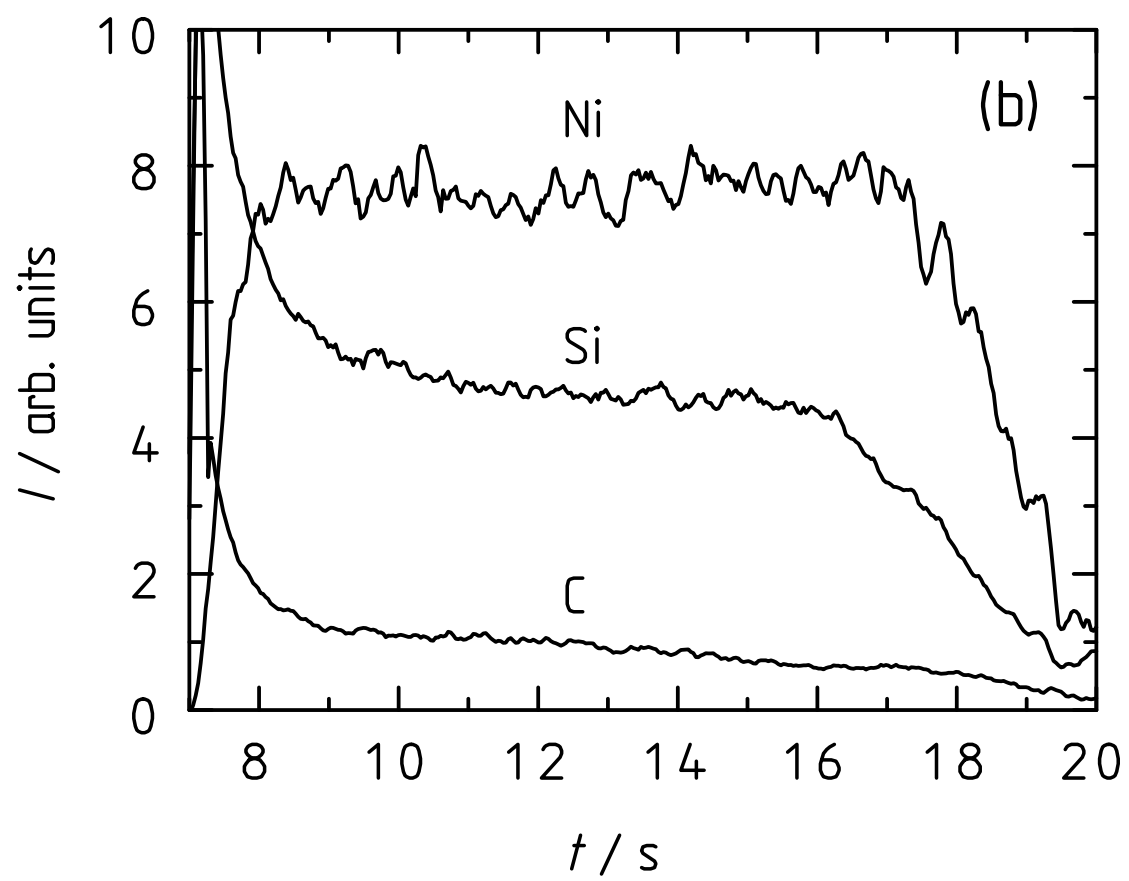


Fig. 2b

This figure "fig_03.gif" is available in "gif" format from:

<http://arxiv.org/ps/cond-mat/9812106v3>

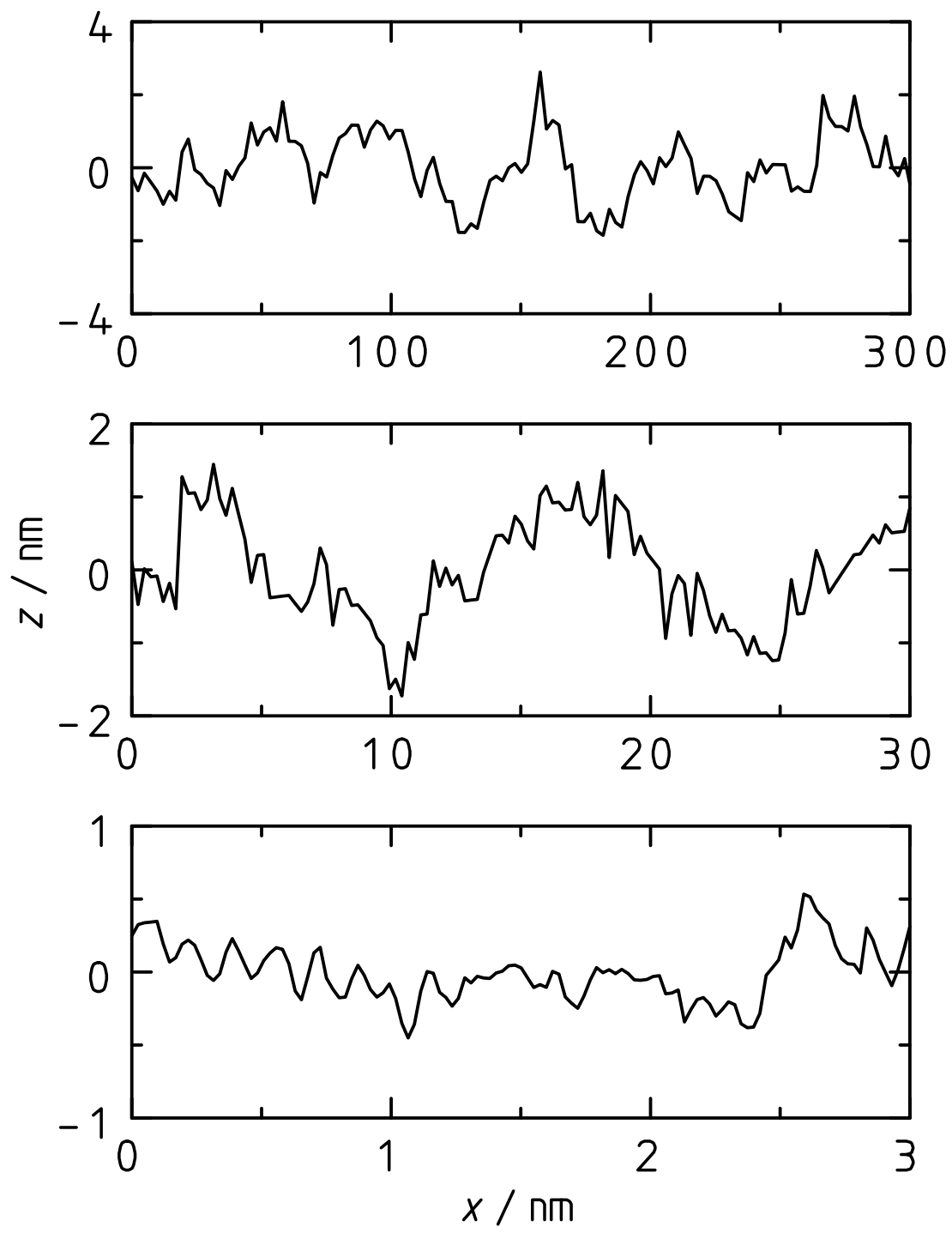


Fig. 4

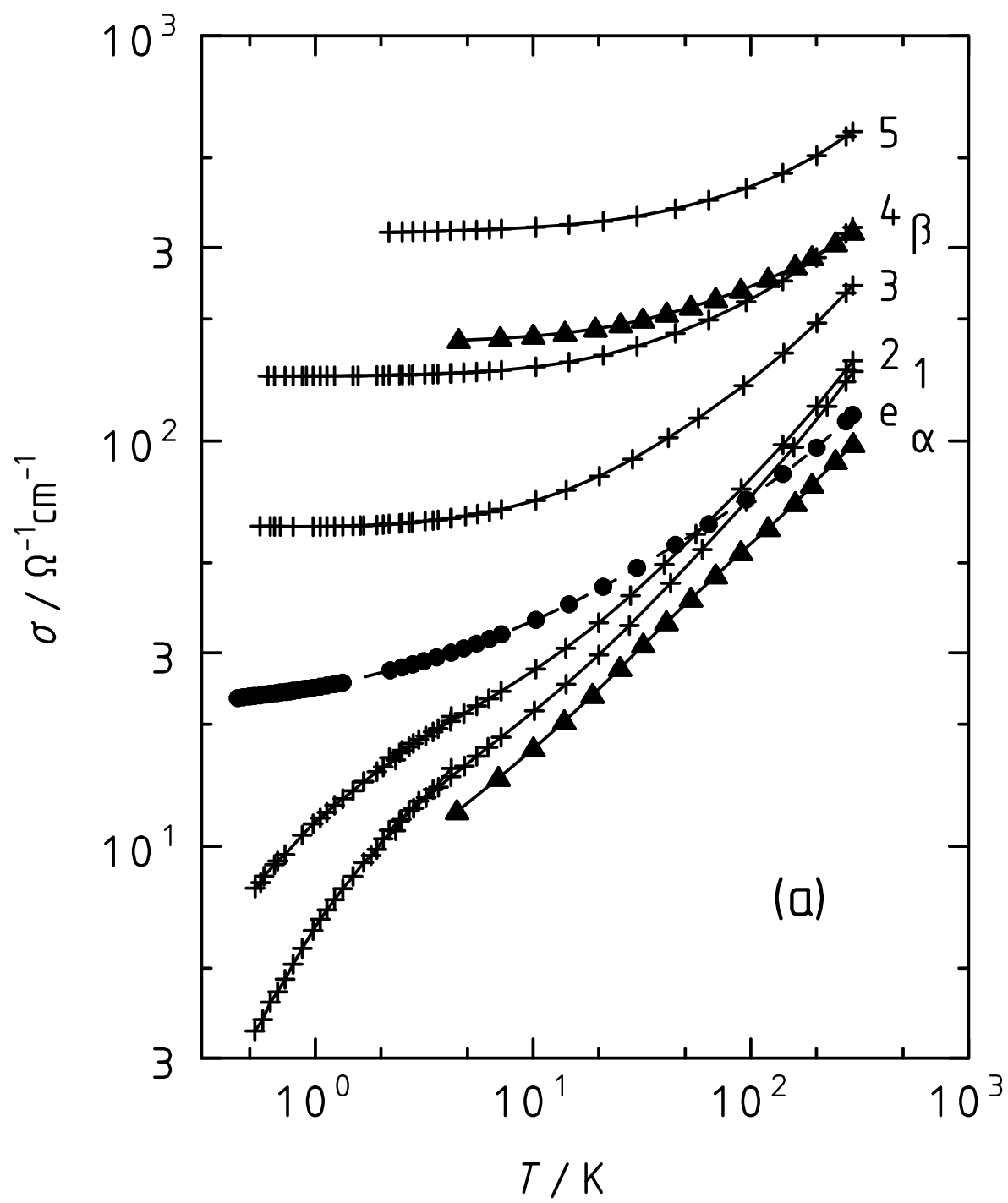


Fig. 5a

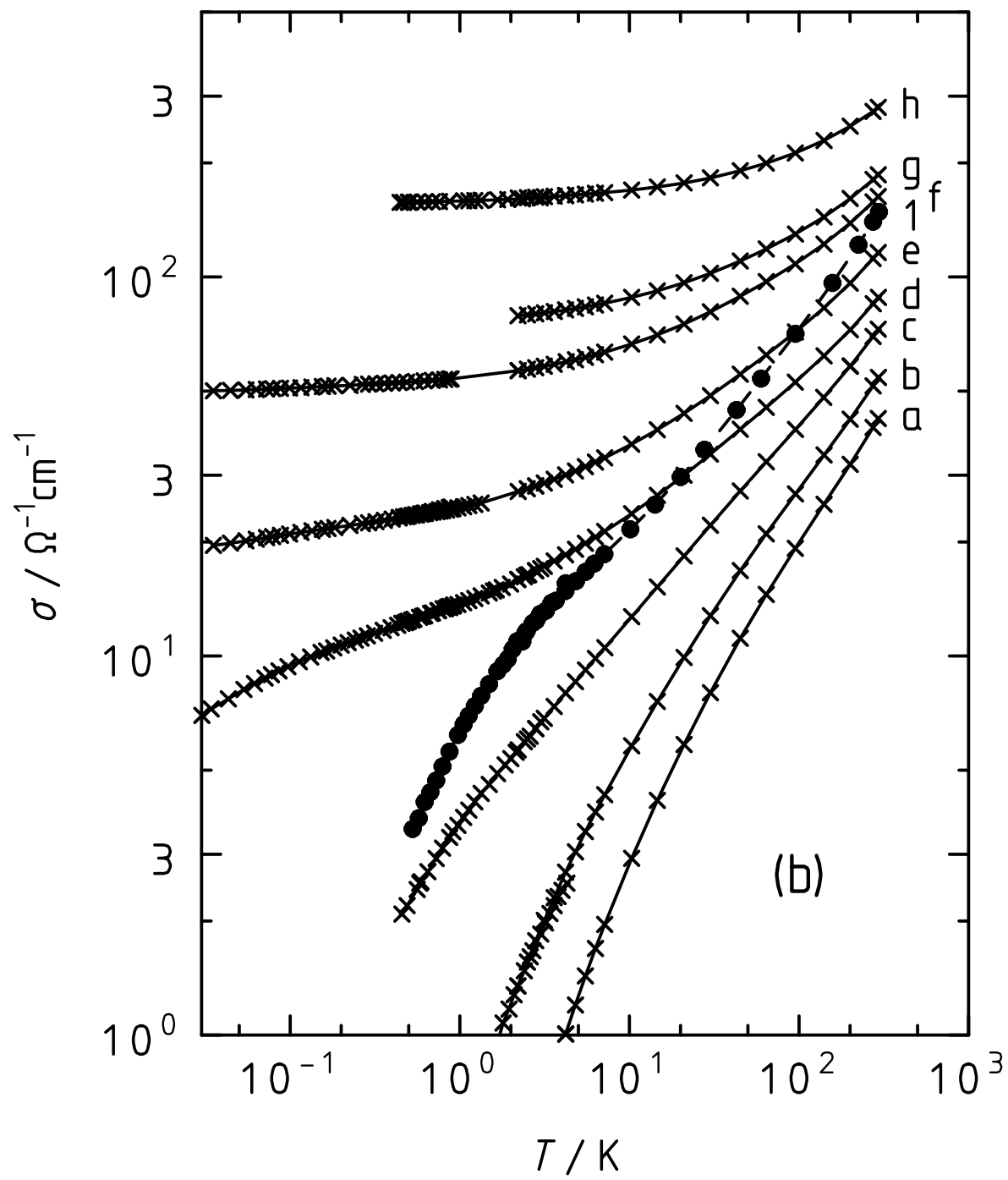


Fig. 5b

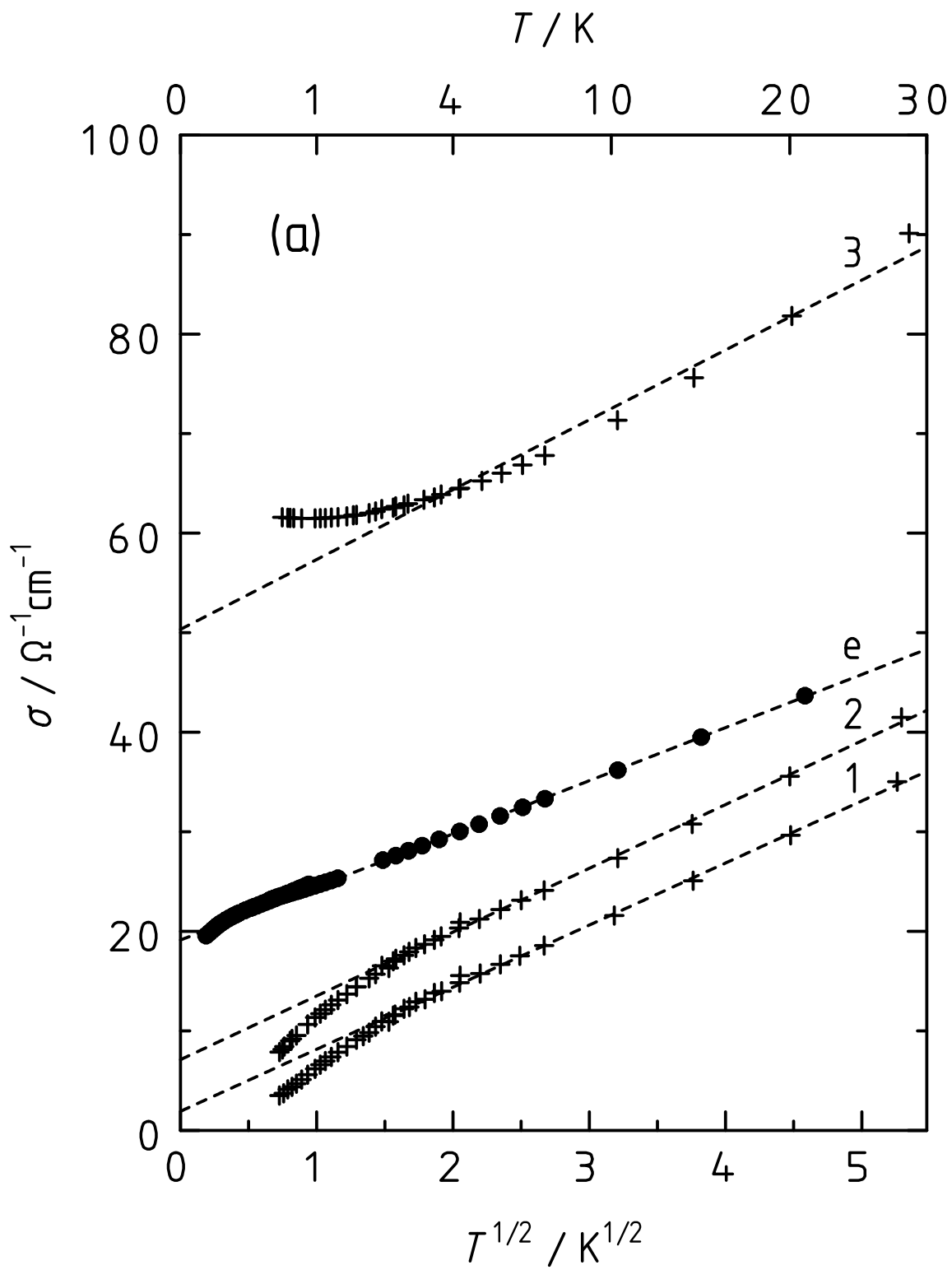


Fig. 6a

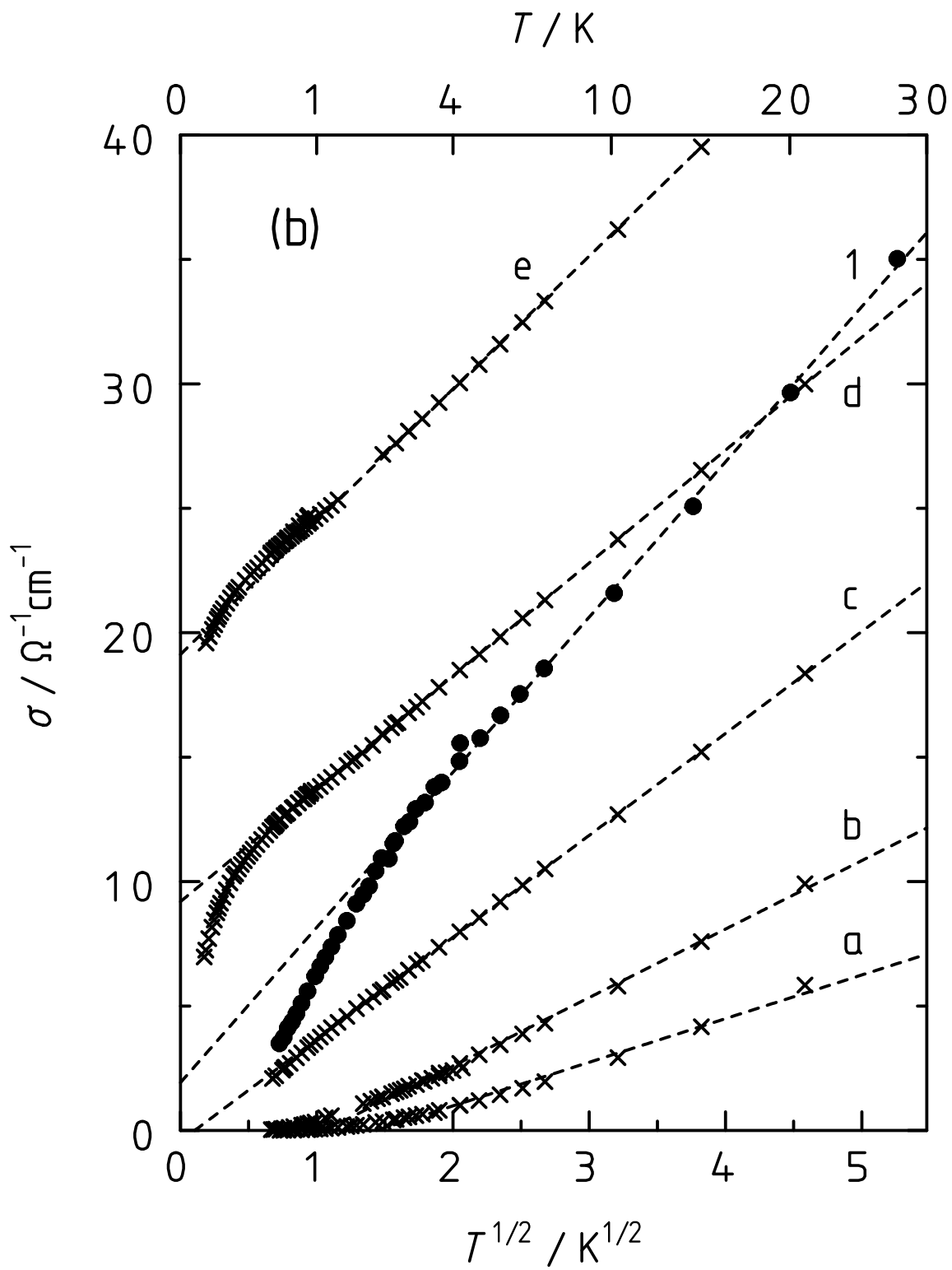


Fig. 6b

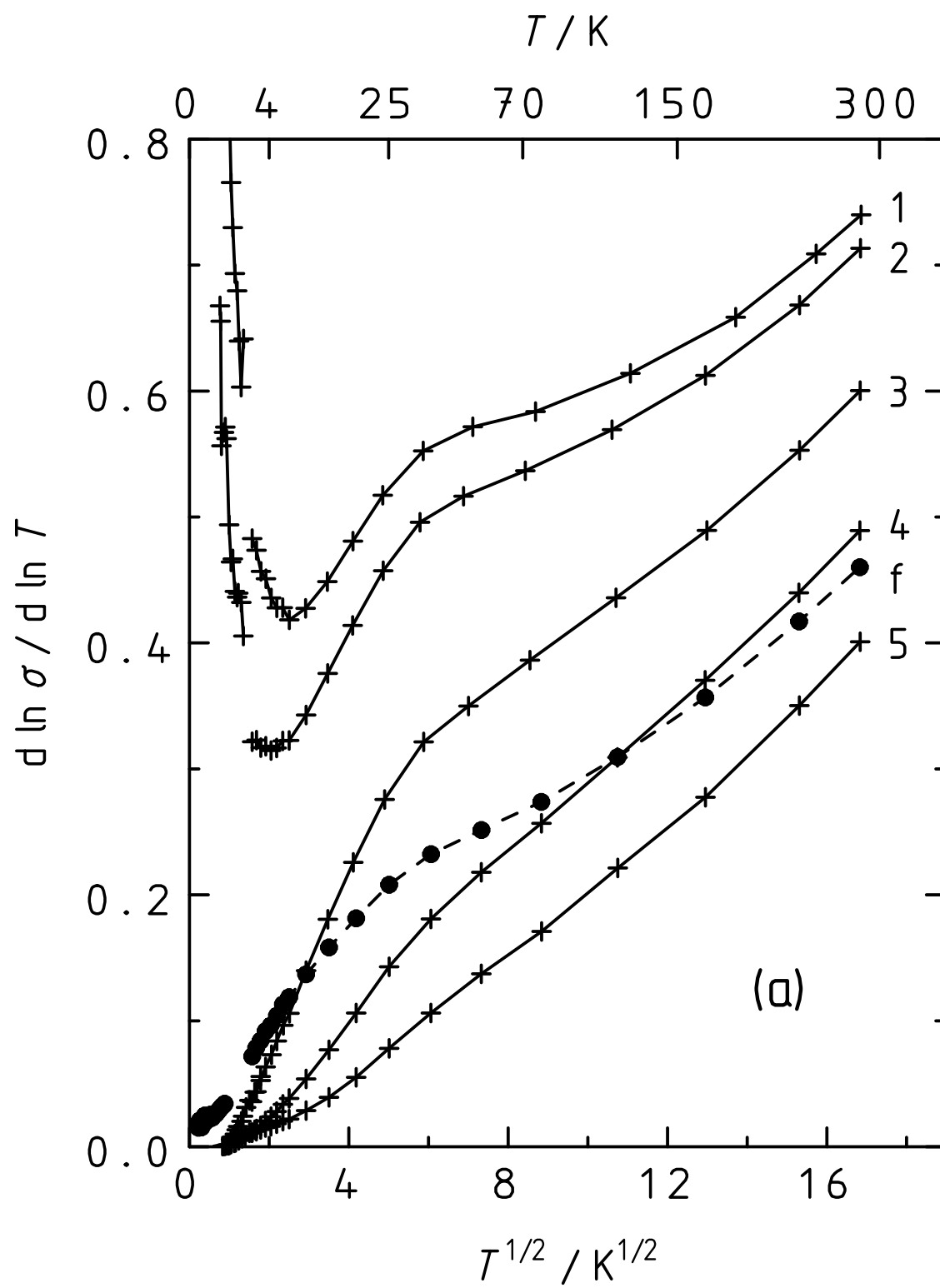


Fig. 7a

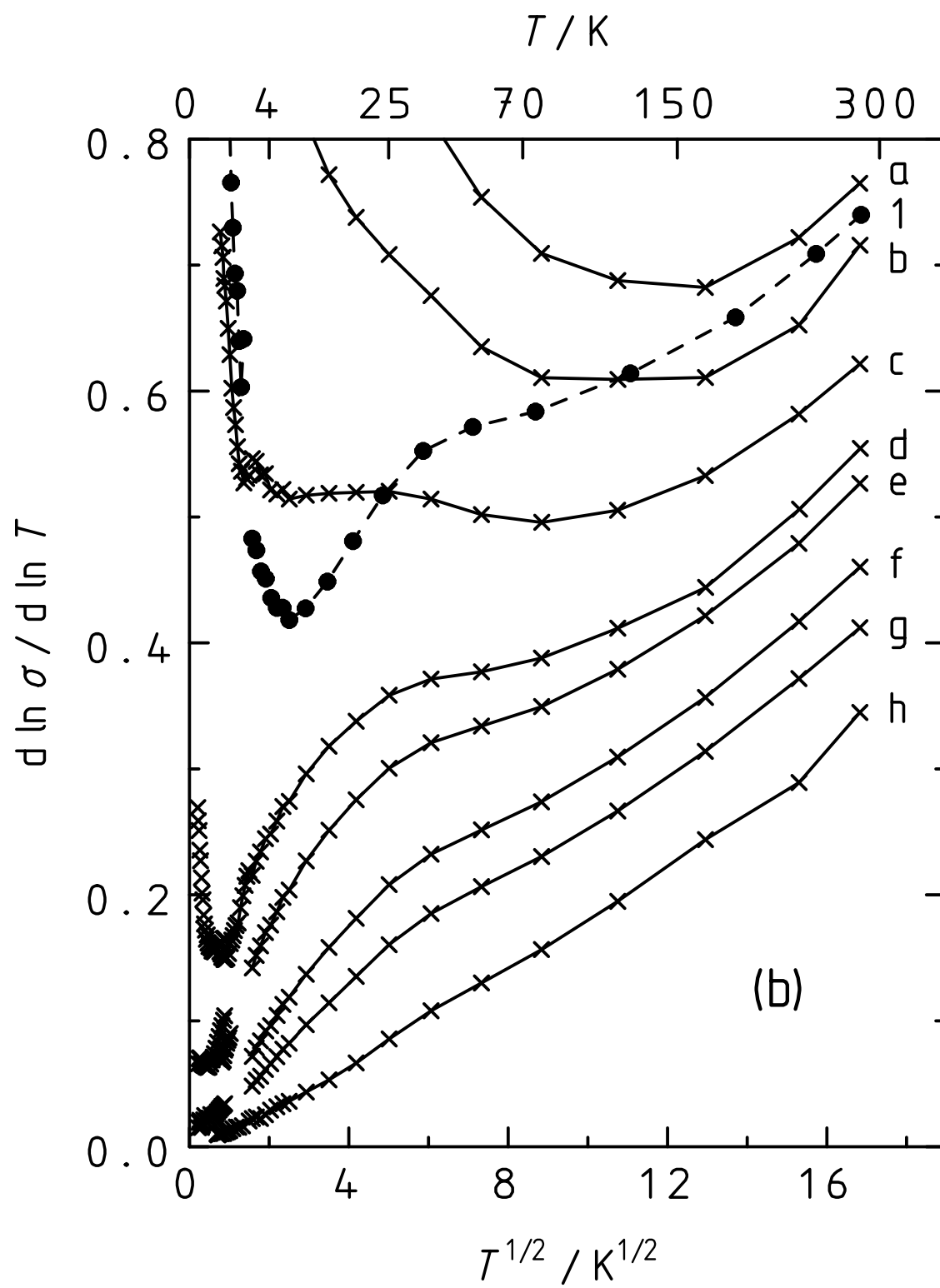


Fig. 7b

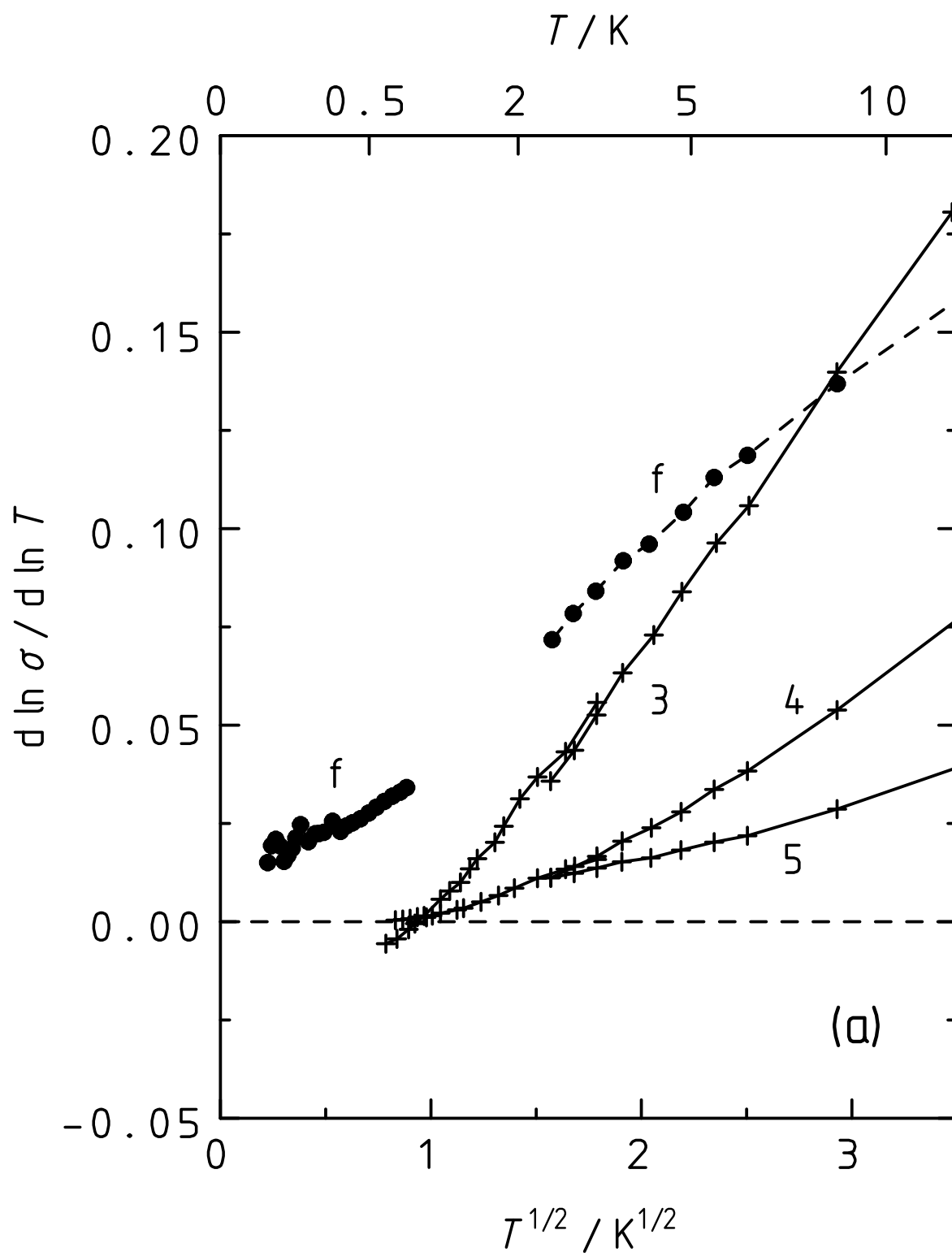


Fig. 8a

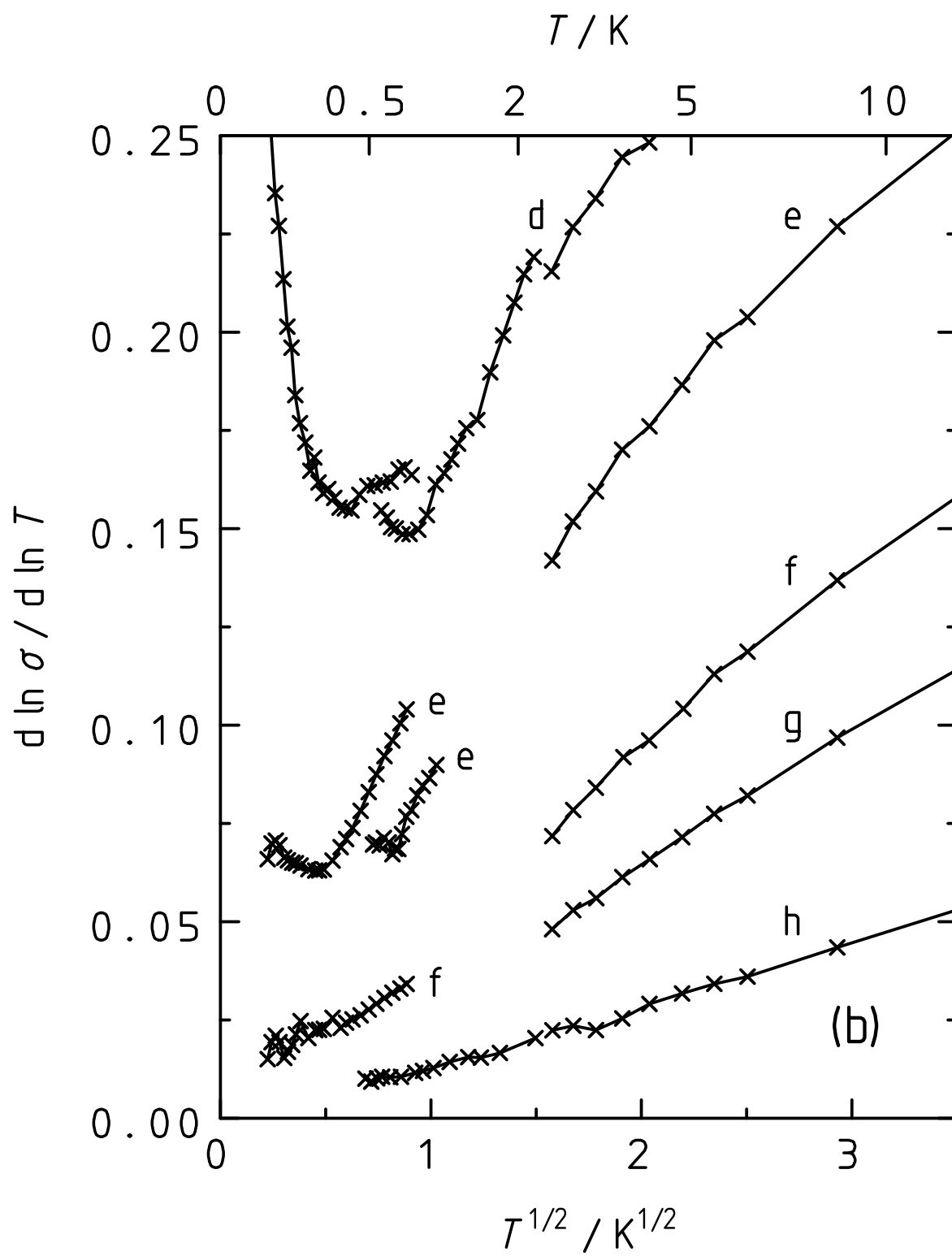


Fig. 8b

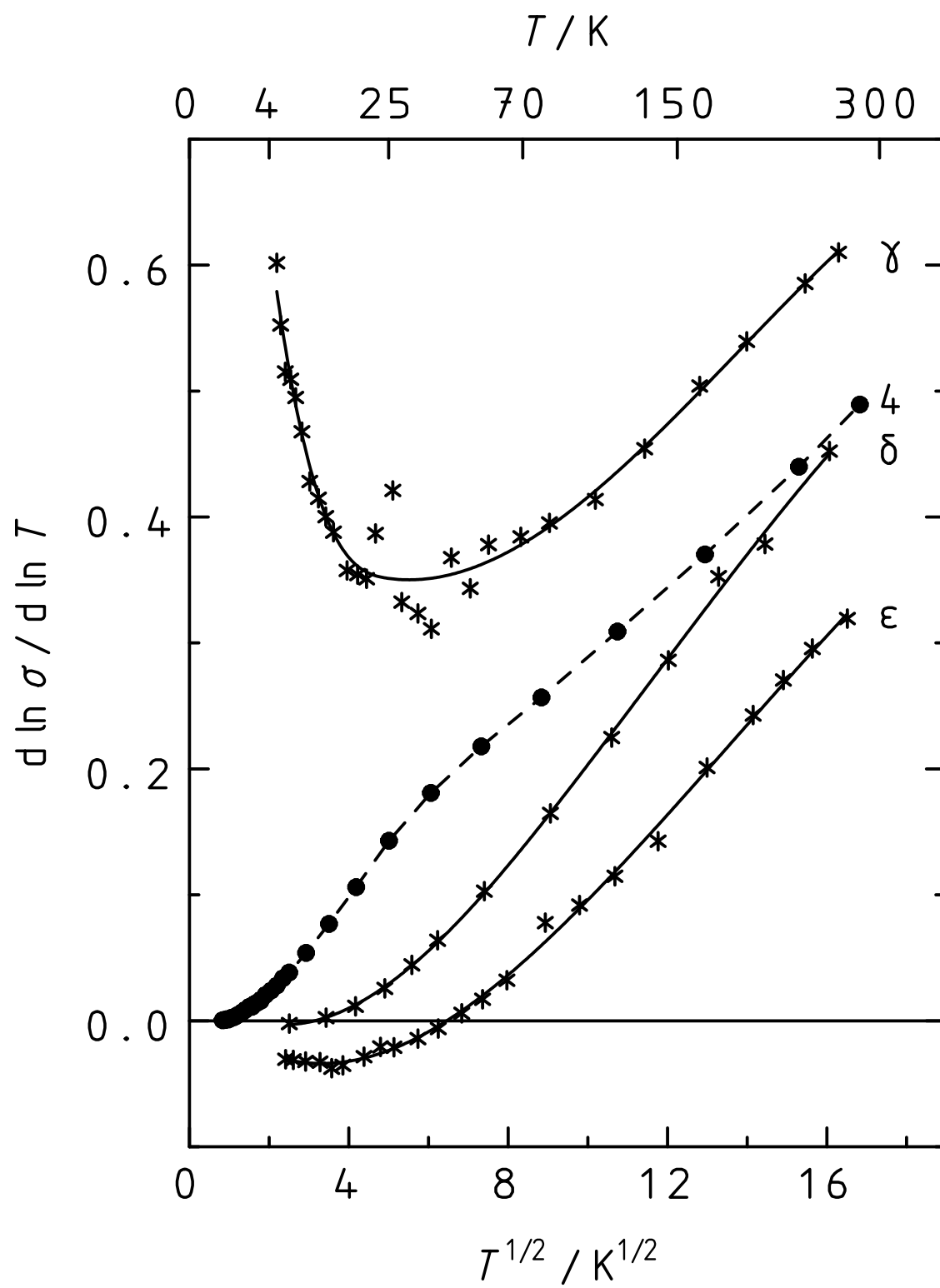


Fig. 9

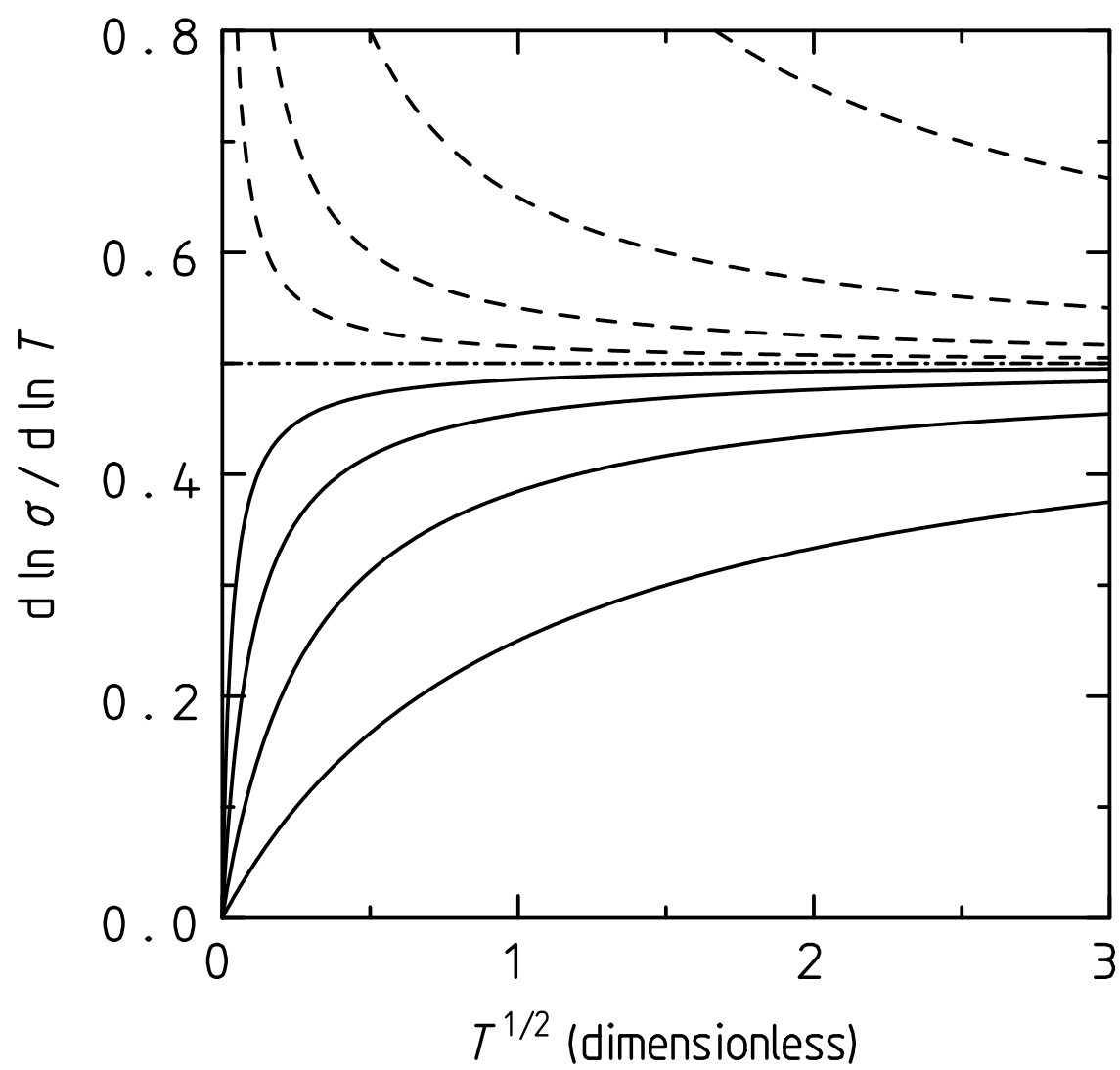


Fig. 10

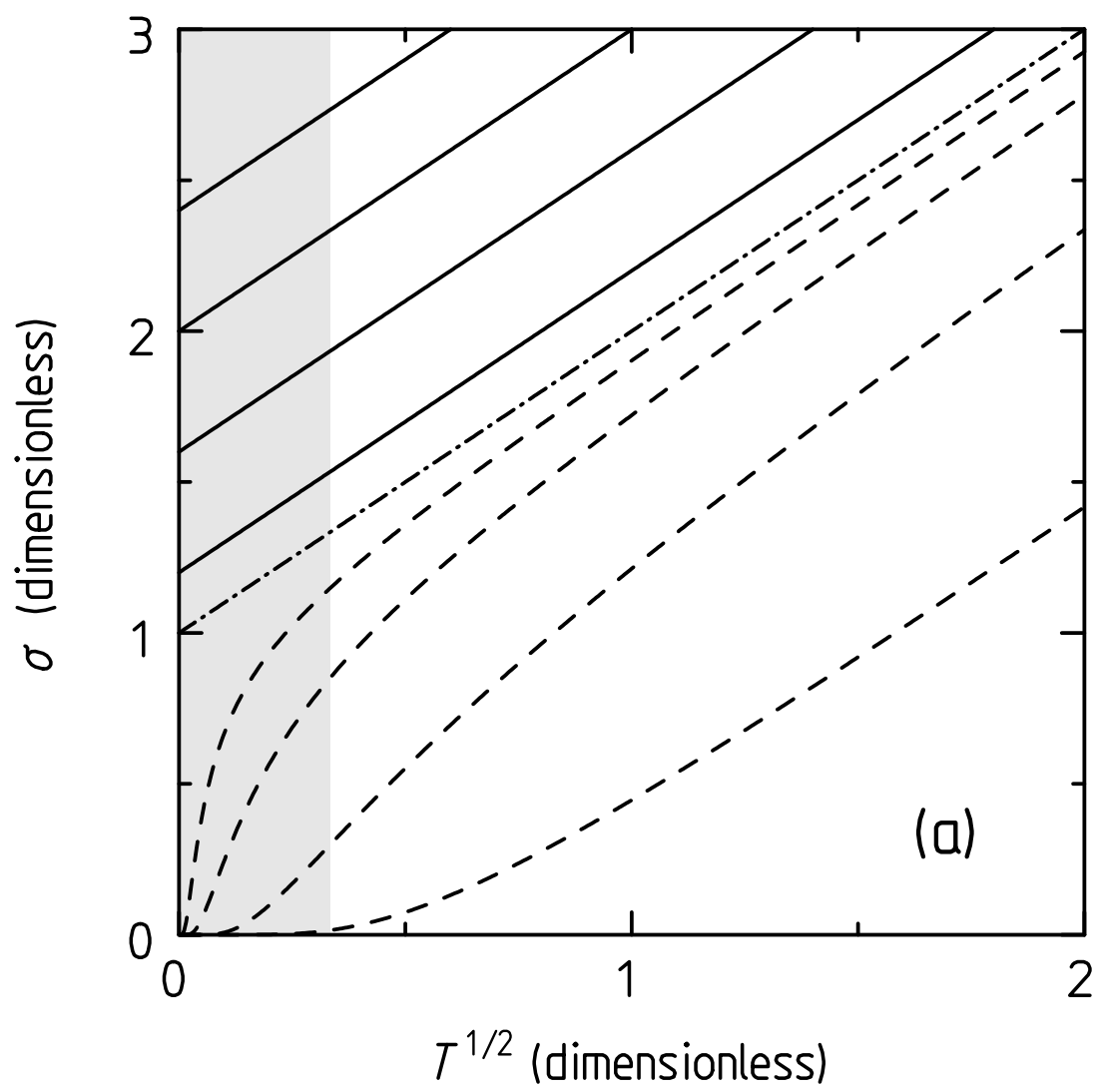


Fig. 11a

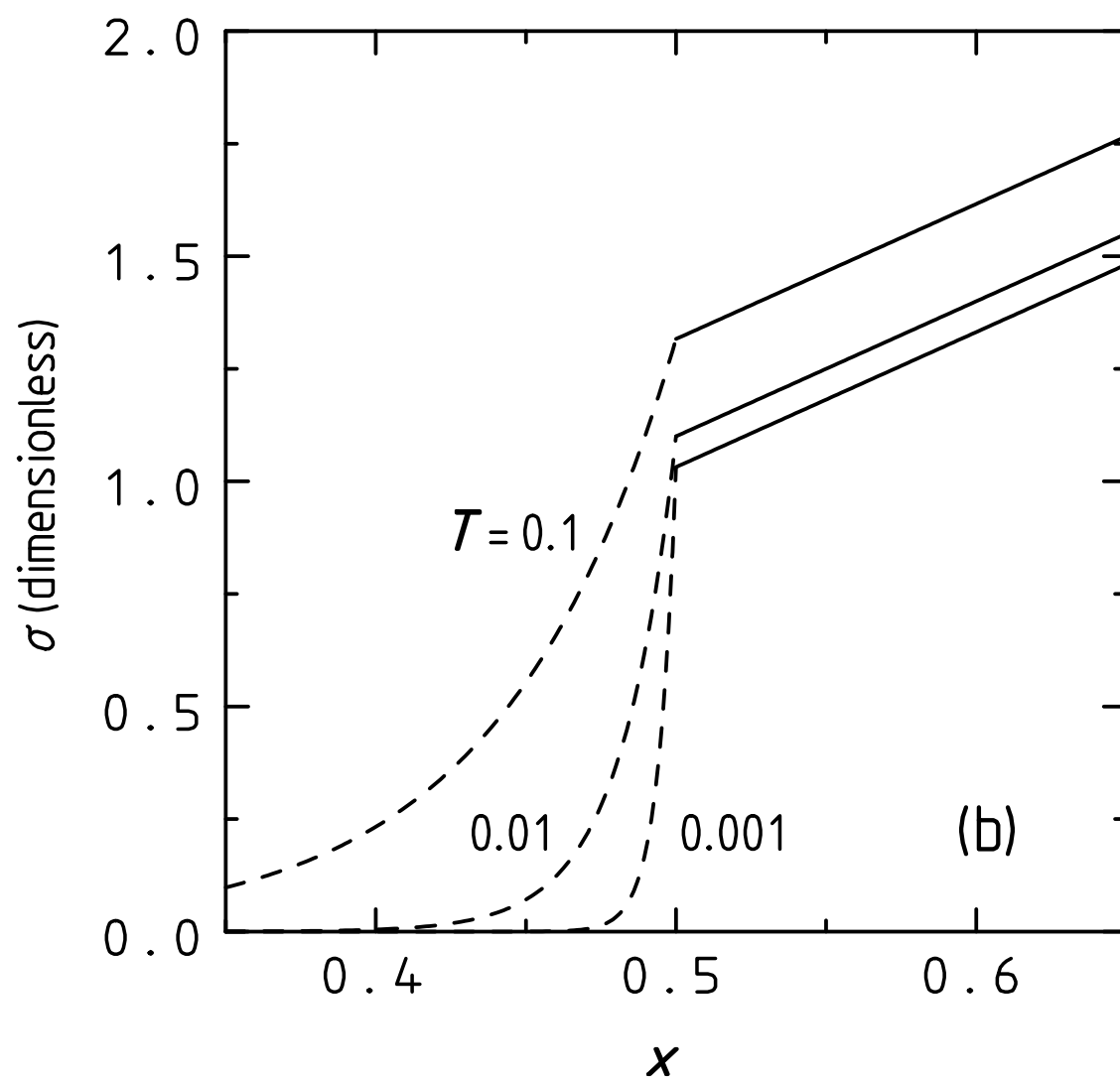


Fig. 11b

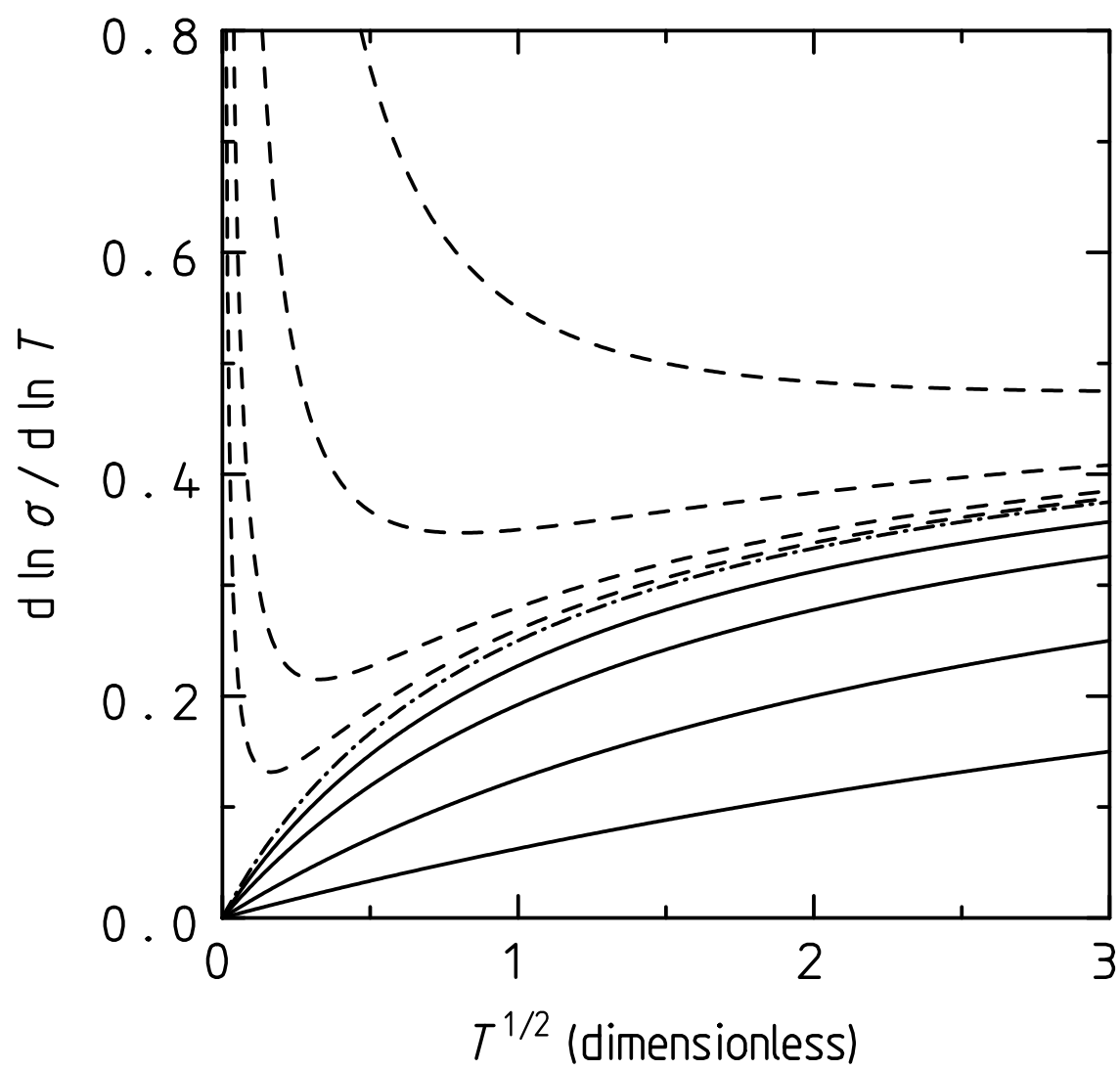


Fig. 12